# MICROELECTRODE ELECTRODE ARRAY STUDIES OF SPINAL MOTOR NEURONS

by

ARUMUGARAJAH THARANEETHARAN

A DISSERTATION

Submitted in partial fulfillment of the requirements
For the degree of PhD in Neuroscience in
the Biology Graduate Program of
Delaware State University

DOVER, DELAWARE
August 2019

This dissertation is approved by the following members of the Final Oral Review Committee:
Dr. Melissa Harrington, Committee Chairperson, Department of Biology, Delaware State University
Dr. Murali Temburni, Committee Member, Department of Biology, Delaware State University
Dr. Michael Gitcho, Committee Member, Department of Biology, Delaware State University
Dr. Hakeem Lawal Committee Member, Department of Biology, Delaware State University
Dr. Rhonda Dzakpasu, Committee Member, Department of Phyiscs, Georgetown University

## DEDICATION

This dissertation is dedicated to my parents Arumugarajah and Mahesaranee, for their unwavering support throughout my life. This dissertation is dedicated to my wife Parvathi, who stood by my side during my darkest hours. This dissertation is dedicated to my children Shiva and Vishnu, who have been my driving force and endless source of joy and happiness through difficult times.

**Microelectrode Electrode Array Studies of Spinal Motor Neurons**

**Arumugarajah Tharaneetharan**

**Faculty Advisor: Dr. Melissa Harrington**

## ABSTRACT

Co-cultures are a traditional method for studying the cellular properties of cell to cell interactions among different cell types. How network properties in these multicellular synthetic systems vary from monocultures are of particular interest. Understanding the changes in the functional output of these *in vitro* spiking neural networks can provide new insights into in vivo systems and how to develop biological system models that better reflect physiological conditions - something of paramount importance to the progress of synthetic biology. Culture models of spinal motor neurons have been customarily studied as a monoculture, and the overwhelming consensus is that in culture they are different in nature from their *in vivo* counterparts. I studied the electrophysiological properties of spinal ventral horn networks cocultured with myocytes or astrocytes using a 64 channel microelectrode array system to record extracellular voltage measurements. When compared over a period of 40 days, significant differences were found between coculture types in metrics of spiking, bursting, and network bursting. Myocyte cocultures, when compared with simple ventral horn cultures, showed significant decreases in spikes, spike amplitudes, spike energy, number of units in network burst, and an increase in interspike interval. Astrocyte cocultures, when compared with simple ventral horn cultures showed decreases in sorted units, burst duration, mean interspike interval, and network burst

duration but increases in spikes, energy of spikes, bursts, spikes per burst, network bursts, and number of units per network burst. This suggests that traditional culturing techniques involving a uniform cell type might not be the best way to functionally model *in vivo* neural networks. Concerning an *in vitro* model system for lower motor neurons, the most accurate model would most likely be a combination of spinal motor neurons cultured with myocytes as well as increased levels of astrocytes. A synthetic ecosystem of various cell types is beneficial to replicating cell behavior *in vitro*, thus is a necessary refinement to the commonly used technique of cell culture. With a more physiological model system, hypotheses about interacting systems can be better addressed and the outcomes will have greater relevancy.

## Table of Contents

## LIST OF FIGURES

LIST OF ABBREVIATIONS

| | |
|---|---|
| AChE | Acetylcholine esterase |
| ALS | Amyotrophic lateral sclerosis |
| ANOVA | Analysis of variance |
| BDNF | Brain derived neurotrophic factor |
| BSA | Bovine specific antigen |
| cAMP | Cyclic adenosine monophos |
| ChAT | Choline acetyltransferase |
| ChR | Channel Rhodopsin |
| CMOS | Complementary metal oxide semiconductor |
| CNTF | Ciliary neurotrophic factor |
| DIV | Days in vitro |
| ESC | Embryonic stem cell |
| EYFP | Enhanced yellow fluorescent protein |
| GABA | Gamma Aminobutyric Acid |
| GDNF | Glial derived neurotrophic factor |
| GI | Gastrointestinal |
| HBSS | Hank's balanced salt solution |
| HiPSC | Human induced pluripotent stem cell |
| IGF | Insulin like growth factor |
| iPSC | Induced pluripotent stem cell |
| ISI | Interspike interval |
| MANOVA | Multivariate analysis of variance |

| | |
|---|---|
| MEA | Microelectrode arrays |
| NMJ | Neuromuscular junction |
| NVU | Neurovascular unit |
| PCA | Principal component analysis |
| PLS | Primary lateral sclerosis |
| SBMA | Spinal-bulbar muscular atrophy |
| SMA | Spinal muscular atrophy |
| SMN | Spinal motor neuron |
| TPP | Triphenylphosphine |
| TTX | Tetrodotoxin |

## CHAPTER I: INTRODUCTION

Neuronal cell culture has been part of the repertoire of techniques used in scientific investigation for almost 75 years (Weiss, 1945). Cell culture in general has been, and continues to be, a valuable tool in isolating and modeling systems. It is a powerful technique when examining specific mechanisms in distinct cell types. What is of special interest when studying within *in vitro* or *in silica* systems is how accurately these synthetic neurobiological models recapitulate the events and processes the researcher is trying to investigate.

Monoculture, the culture of a single cell type, has been the typical mode for cell culture up until recently. However, interest in investigating the interactions between cell types have paved the way for new advancements such as semipermeable membrane well inserts, which allow various cell types to share media but never have direct contact, or separate chambers connected by microfluidic systems, allowing for cells to contact other cell types in an extremely controlled fashion (Aebersold et al., 2018; Silva, Santos, Leng, Oliveira, & Amédée, 2017). The growing literature on research using cocultures suggests that monoculture may not be painting an accurate picture of the systems being modeled. Intercellular interactions and communication are necessary components of cellular networks, underlying initiation, promotion, and progression (Bahmani, Taha, & Javeri, 2014; Hyung et al., 2015; Im, 2014; Krencik et al., 2017; Miki et al., 2012).

It is common amongst biologists to classify cells using cellular and/or molecular markers. Real time functional assays of many cellular functions are difficult and costly, so inference of cellular function through expression of genetic markers makes for a convenient way to differentiate cell types. However, this maybe a misleading, particularly in the case of neurons. For example, the NSC-34 motor neuron hybridoma shows many of the molecular characteristics

of a motor neurons however it is an inadequate model for glutamatergic excitotoxicity (Mavel et al., 2016). Neuronal function, and thus a neuron's classification, may be more accurately represented by its electrical and synaptic activity which are relatively easy to measure in real time. How well do cultured neurons mimic the behavior of neurons in neural tissue? This picture can be more clearly painted through electrophysiology.

The gold standard for determining the functional output of neurons is measuring their electrophysiological properties. Single cell intracellular patch clamp recording is the foundation of much of the rich history of electrophysiology in neuroscience. However, intracellular patch recording has two major deficits when examining a neural network. The first deficit is difficulty in understanding at the activity of the larger network. From a single electrode network activity can only be inferred, not measured. Multiple electrodes can be patched to different nodes of a network, but with each additional cell patched the difficulty and complexity of the experiment increases exponentially. The second deficit is the inability to look at long term recordings. Neural networks are dynamic entities that evolve over time. Patching a neuron is a traumatic event that punctures a hole in the membrane and dialyzes the cytoplasm, after which viability becomes progressively limited. Intracellular recording can only really be done as an end stage experiment. However, recent advancements in material sciences for simple electrode and complementary metal oxide semiconductor (CMOS) technologies has allowed major advances in extracellular field potential recording using microelectrode arrays (Amin et al., 2016; Yada, Kanzaki, & Takahashi, 2016). Besides network spatial resolution, microelectrode arrays (MEAs) also have an advantage of allowing long term recordings. For *in vitro* experiments, cell culture on MEA probes can be returned to an incubator after recording and be recorded again days or weeks later. Similar situations exist for *in vivo* MEAs. A recent collaboration by BrainGate has

demonstrated a brain computer interface with a 96 channel MEA implanted in human patients that was stable for a half year (Milekovic et al., 2018).

We are using a multielectrode approach to examine the functional output of ventral horn neurons when cocultured with two of their most influential partners, astrocytes and myocytes. We used ventral horn neurons, because this is the primary location of motor neurons. Neurons are usually isolated from astrocytes before culturing, as in our case using a density gradient. As the importance of astrocytes to the function of neural networks has become increasingly clear in recent literature, this was the primary choice when choosing a cell type to coculture with ventral horn neurons. With the exponential growth in research related to astrocytes and the neurovascular unit (NVU) since the Stroke Progress Review Group meeting in 2001, our understanding of these cells - once thought of as almost a purely structural support cell with some immunological functions - has evolved into recognizing their role as calcium based parallel co-processors (field programmable gate array) integral to most neural networks (Haghiri, Ahmadi, & Saif, 2017; Iadecola, 2017). In order to achieve a model that replicates an *in vivo* neural system more closely than a monoculture, it seems highly likely that astrocytes will be an essential component. Our second choice was due to the specific nature of our neurons of interest, motor neurons. Since skeletal muscle is the major end target of spinal motor networks, coculturing our ventral horns neurons with myocytes was a logical option. We also have great interest in producing an accurate primary motor neuron model in a reproduceable fashion. It has been shown that almost any neuron will form a neuromuscular junction (NMJ) with skeletal muscle cells in culture (Demestre et al., 2015; Jevsek, Mars, Mis, & Grubic, 2004; Liu et al., 2011). The resulting NMJ formation leads to an increase in acetylcholinesterase subsequently increasing acetylcholine, the major neuromuscular neurotransmitter (Jevsek et al., 2004; Jiang et

al., 2003). Determining how the overall network activity of spinal cultures might be affected by these changes has yet to be examined.

## CHAPTER II: LITERATURE REVIEW

### *2.1. Spinal Motor Neurons*

Spinal motor neurons (SMNs) are affected in disorders such as amyotrophic lateral sclerosis (ALS), primary lateral sclerosis (PLS), spinal muscular atrophy (SMA), and spinal-bulbar muscular atrophy (SBMA). Modelling spinal motor neurons *in vitro* and assessing the network output has been challenging for several reasons. Motor neurons are fragile and have difficulty recovering from traumatic events. Mature motor neurons possess a dense dendritic arborization (M. D. Kim, Wen, & Jan, 2009) whose injury initiates cell death (Fogarty, Mu, Noakes, Lavidis, & Bellingham, 2016). Immature motor neurons are harvested from embryos for modelling motor neuron diseases because of their increased viability, although motor neuron diseases frequently have a mature onset. Spinal motor neurons *in vivo* mature down a path delineated by the surrounding cell types. Replicating these intercellular relationships to produce an accurate *in vitro* model has proved a formidable task. Network activity has been difficult to assess using older electrophysiological techniques, namely single cell patch clamp, because of the limited number of recording channels while newer techniques such as multielectrode arrays have concerns with electrode sensitivity, probe impedance, and signal noise.

When studying spinal motor neuron studies *in vitro* investigators have used cell lines, stem cells, or primary spinal motor neurons harvested from embryos. The stem cells most commonly used are mouse embryonic stem cells (ESCs) or human induced pluripotent stem cells (iPSCs). Of those options, iPSCs have had the greatest trending interest recently because they are the only source of studying patient derived motor neurons. Because these iPSCs are harvested from humans, they have the greatest potential for translational research but also a very limited supply resulting in increased costs. A typical protocol for production of motor neurons from

human iPSCs takes 35 days, with 5 variations in media, selection based on 5 markers, and approximately 45 steps (Hu & Zhang, 2009). The complexity and duration of such an endeavor lends itself to error. Using patch clamp recordings, portrayed in Figure 1, it has been shown that iPSC derived motor neurons show similar electrophysiological properties to functionally mature motor neurons (Pfaff et al., 2011), typically based upon fast inactivating current eliminated by tetrodotoxin (TTX) and repetitive action potential firing following current injection (Davis-Dusenbery, Williams, Klim, & Eggan, 2014). However, there is a great divide between expressing typical currents, firing induced action potentials and developing activity characteristics of motor neurons *in vivo*.

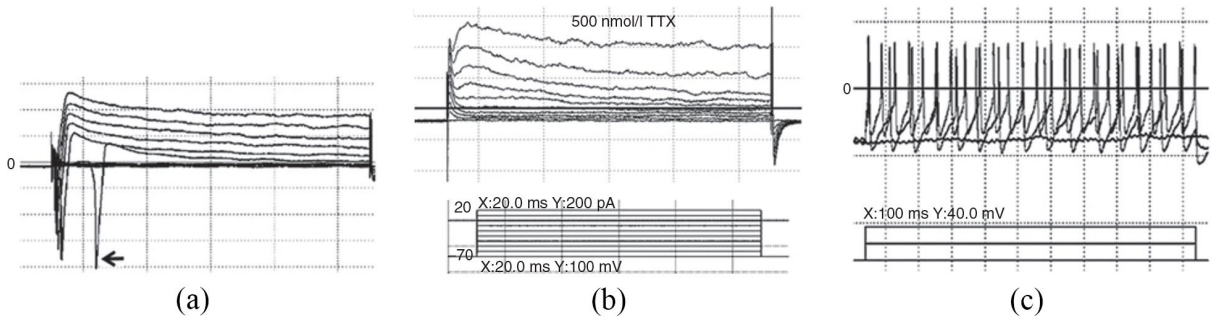


(a) (b) (c)

**Figure 1.** Electrophysiological activity of iPSC derived motor neurons. (a) Strong sodium current activity in induced motor neuron shown by arrow. (b) Sodium channel current were blocked by tetrodotoxin. (c) Electrical stimulation induced action potential, indicating functional maturity. (Pfaff et al., 2011)

Spontaneous firing is requisite in establishing a functional neural network, while synchronous firing across multiple neurons is a sign of an established network. Spontaneous firing is a precursor to synaptic connectivity, along with dendritic arborization and functional synapses. The initiation of spontaneous firing falls under two main categories. A neuron will fire spontaneously due to intrinsic conductance properties or it may fire due to synaptic and non-synaptic excitation. When examining *in vitro* systems, intrinsic conductance properties and non-synaptic excitation can occur immediately after plating however synapses take time to develop.

Spontaneous activity in developing cerebellum can occur in the absence of synaptic input amongst dissociated Purkinje cells. This phenomena has been isolated to fluctuating $Na^+$ currents mediated by Nav 1.6 and fluctuating $K^+$ conductances mediated by Kv3.3 (Akemann, 2006; Grieco, 2004; Kerschensteiner, 2014; Raman & Bean, 1997).

Modulation of spontaneous activity can also be nonneuronal in origin. Patch clamp recordings of acute spinal slices from embryonic mice demonstrate spontaneous activity as early as E11.5, while first synaptic activity doesn't develop till E12.5. At E12.5, spontaneous activity unresponsive to gabazine or TTX is blocked by glycernergic antagonists (Fig. 2). Between the ages of E12.5 and E14.5 the main source of glycine in the embryonic spinal cord is radial glial cell progenitors, which help in neuronal migration. Radial cells also release glycine during synaptogenesis, as well as during mechanical stimulation through volume sensitive chloride channels (Fig 3). Most importantly during development, glycine release upregulates spontaneous activity by depolarizing immature neurons (Scain et al., 2010).

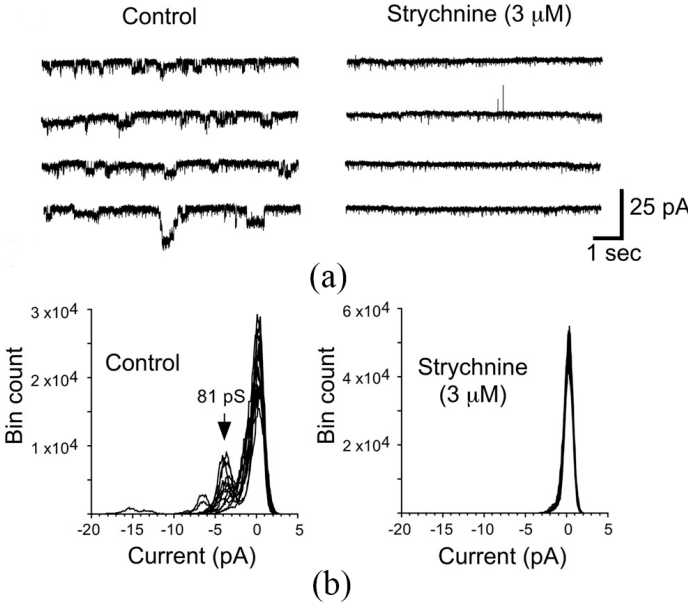


**Figure 2.** Spontaneous activity in murine slices. (a) Spontaneous single channel activity in E12.5 lumbar motor neurons are blocked by strychnine, demonstrating glycernergic receptor activation. (b) Amplitude histogram of superimposed channel openings before and during strychnine application (Scain et al., 2010).

Further down the motor pathway, motor neurons *in vivo* have synaptic mediation of spontaneous activity through cholinergic and GABAergic inputs that are most likely autocrine in

origin. Chick lumbosacral motor neurons at embryonic day 4, shortly after exiting the spinal cord but still not having reached their target muscles, show highly patterned spontaneous activity. The dominant neurotransmitter involved in driving activity is acetylcholine, unlike older spinal motor circuits which are driven by glutamate. Using a whole cord prep and suction electrodes, cholinergic antagonists are able to block spontaneous firing, but after recovery it will become driven by GABAergic inputs. Although it has long been thought that spontaneous activity was purely method for refining synaptic connections, the early occurrence of spontaneous firing suggest that it may have a role in pathfinding or spinal motor circuit formation (Milner & Landmesser, 1999)..

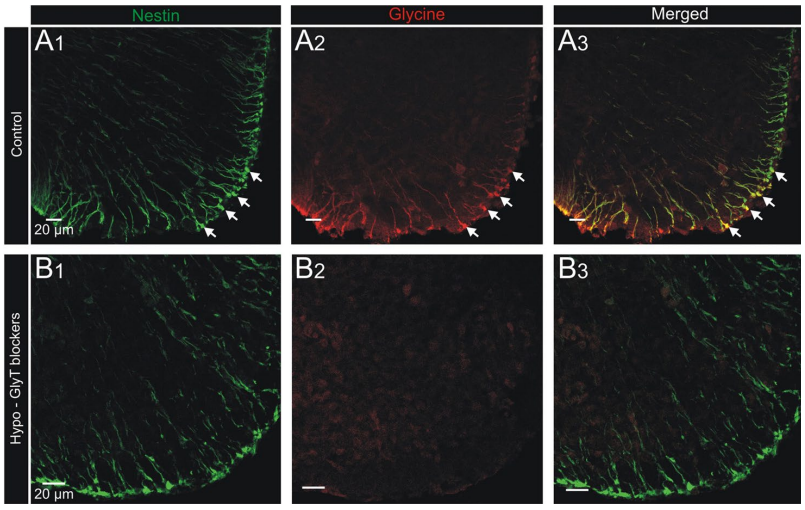


**Figure 3.** Glycinergic activity in radial cells. (a1-a4) Radial cells from E12.5 embryonic mice release glycine (b1-b4) Glycine release by radial cells in embryonic mouse spinal cords is blocked by glycine membrane transporter blockers.

Human stem cell derived motor neurons show a continuous increase in number of dendritic branches and total outgrowth as they mature (Takazawa et al., 2012), which is seen up until E13 in mice but starts to decrease at E15. The resting membrane potential is slightly depolarized and the input resistance is several times higher than *in vivo*. The combination of these two electrophysiological characteristics results in a cell that is hyperexcitable, but has difficulty firing spontaneously (Takazawa et al., 2012). Interestingly, motor neurons derived from human ALS subjects have almost twice as much spontaneous firing as motor neurons

derived from control subjects (Wainger et al., 2014). It has also been suggested that pluripotent stem cell derived motor neurons have few interneural synapses (Sances et al., 2016), while others have shown that embryonic stem cell derived motor neurons can form neuromuscular junctions (Umbach, Adams, Gundersen, & Novitch, 2012), although this characteristic is not unique to motor neurons. If embryonic stem cells are cocultured with astrocytes (Fig. 4) then there is an increase synaptic formation, synaptic activity, and a corresponding increase in spontaneous activity that bring it more in line with developing motor neurons *in vivo.* (Johnson, Weick, Pearce, & Zhang, 2007). At the gross level, stem cell and iPSC-derived motor neurons may appear to be forming active networks with dendritic arborizations, but they may lack the ability to spontaneously fire and have limited potential to pass that signal via a synapse.

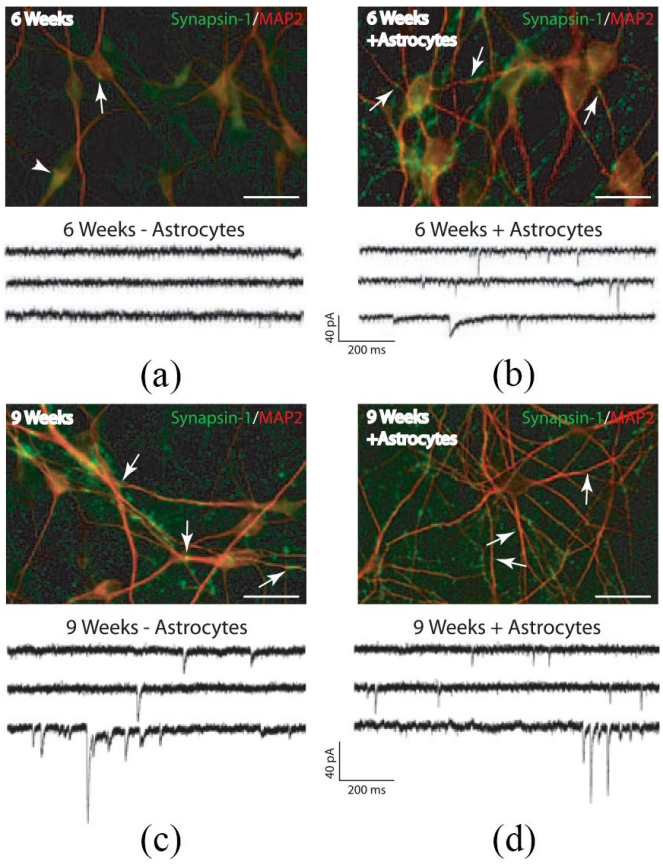


**Figure 4.** Stem cell and astrocyte coculture. In human embryonic stem cell derived neural progenitors generated neurons grown at 6 weeks *in vitro* without astrocytes (a) show little synapsin immunoreactivity and little spontaneous electrical activity. If those same neurons are grown in contact with astrocytes (b) then synaptic presence as well as spontaneous activity increases. Although synapses and spontaneous activity are seen in 9 weeks *in vitro* (c), synapsin is heavily localized around select axons with less frequent firing yet high in amplitude. With astrocyte coculture for 9 weeks (d) there is a more intricate axonal web, more diffuse synapsin localization, and more frequent spontaneous firing (Johnson et al., 2007).

Because of difficulties in harvesting and culturing primary motor neuron cultures, a spinal motor neuron neuroblastoma hybrid cell line, NSC-34, became very popular as an in vitro model for motor neurons (Cashman et al., 1992; Matsumoto et al., 1995). However, it has been recently shown that in the NSC-34 line, there is limited ability to induce glutamate stimulated excitotoxicity, most likely due to decreased sustained calcium entry (Mavel et al., 2016). This deviation from the behavior of motor neuron *in vivo* greatly limits it's use as a model system for studying motor neuron disease, and potentially other aspects of motor neuron physiology. Stem cells and cell lines have their limitations, but if investigations require a homogenous population then these are potential options.

Primary culture has been a staple of motor neuron *in vitro* model system since the late 1960s (S. U. Kim, Oh, & Johnson, 1972; Peacock, Nelson, & Goldstone, 1973; Schlaepfer, 1968). Rat, chick, and mouse embryos have been the most predominant model systems over the years. Although studies with mouse spinal cultures (Peacock et al., 1973) came into the literature soon after rat (Schlaepfer, 1968) and chick (S. U. Kim et al., 1972), they didn't gain much popularity till much later on. In my experience rat and chick spinal motor neurons are more robust, and have greater viability in culture with chick being the easiest to culture. However, the popularity of genetic mouse models has expanded the use of spinal motor neuron cultures of murine origin.

In primary cultures cells can either be dissociated or cultured *in situ*, as in organotypic cultures. When cultured on multichannel microelectrode arrays dissociated cells are more firmly anchored to the probe, as compared to organotypic cultures which tend to move about. When multiple recordings are made over multiple days, dissociated neurons have an advantage because the position of active neurons in relationship to electrode will remain fairly constant. However,

organotypic cultures have the distinct potential to dissect the circuitry of neuroanatomical pathways due to the preservation of spatial relationships an the microenvironment. Organotypic motor neuron cultures also have increased viability as compared with dissociated neurons. Other cell types surrounding the neurons of focus, such as astrocytes, will provide both structural and trophic support. Cells in organotypic cultures aren't forced to undergo the stressors of chemical dissociation usually by trypsinization, and the shear force of physical titration.

*2.2. Coculture*

Another type of dissociated cell culture is a coculture system. Coculture systems involve the mixture of two or more cell types and can be divided into two main families, culture with cell-cell contact or culture without cell-cell contact. In cultures with cell-cell contact there are several techniques to control cell-cell contact including micropatterning, temporary dividers, or a degradable hydrogel. In cultures without cell-cell contact techniques for segregated co-culture include the introduction of conditioned media, a porous membrane hammock, or a permeable hydrogel divider (Bogdanowicz & Lu, 2013). Microfluidic coculture chambers are an interesting hybrid between systems utilizing aspects of both with and without cell-cell contact systems. Although microfluidic chambers have separate microenvironments for different cells, they allow for contact between various chambers in an extremely controlled fashion. Innovated in the late 1970s by using a Teflon divider set over a petri dish with a collagen coated coverslip that was scratched by insect pins. The divider was sealed to the coverslip by sterilized silicon grease, but still allowed for the passage of axons through the scratched grooves (Campenot, 1977). This configuration allows for two different cell types to be grown in two separate microenvironments with discreet contact. It is especially useful when studying neural types with long processes (Fig. 5), and particularly helpful in studying neuromuscular junctions (Ionescu, Zahavi, Gradus, Ben-

Yaakov, & Perlson, 2016; Southam, King, Blizzard, McCormack, & Dickson, 2013; Zahavi et al., 2015). Advancements in motor neuron cultures using microfluidic systems, such as integration with microelectrode array systems, has advanced dramatically over the past several decades.

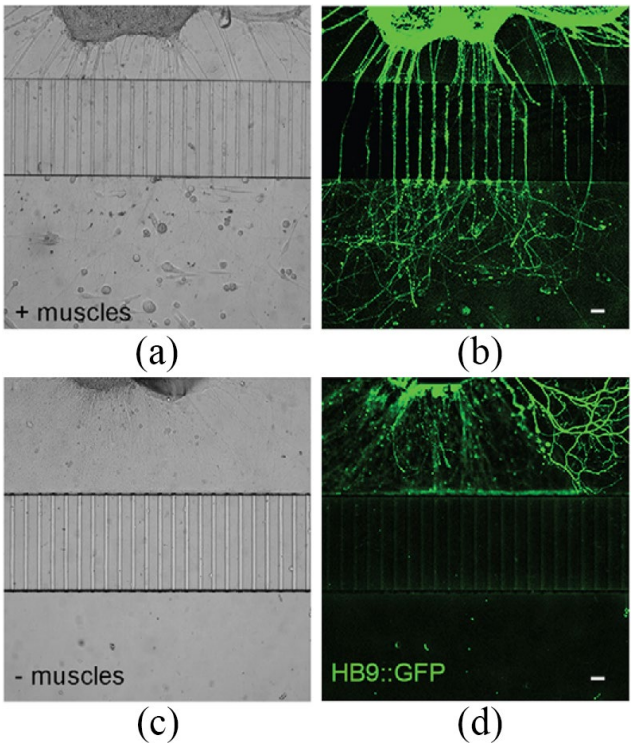


**Figure 5.** Spinal cord and muscle coculture utilizing microfluidic channels. Brightfield images (a & c) and epifluorescent images of spinal cord explants expressing HB9::GFP (b & d) grown by microfluidic channels. Differentiated myotubes are grown adjacent to the spinal explants in top panels (a & b), while no muscle tissue is cocultured in the lower panels (c & d). (Zahavi et al., 2015)

Around the same, in the early 1970s, the first multichannel microelectrode arrays began appearing. Initially the first arrays were platinum and glass insulated and sported a mere four electrodes (Hovey, Bak, & Carpenter, 1972). Later, probes etched from metal films were able to push the electrode count to thirty due to improved fabrication techniques (Thomas, Springer, Loeb, Berwald-Netter, & Okun, 1972). The ease at which etched films could be down scaled in size cemented it as the predominant production process for the next several decades, allowing for the first recordings from dissociated neurons in 1980. It wasn't till the 1990s that research progress began to accelerate with published work using microelectrode arrays in the biological sciences.

*2.3. Multichannel Analysis*

With this increase in interest came the need for more efficient analysis methods. Progress in software always lags progress in hardware. Similarly, progress in the analysis of multiple channels recorded simultaneously was still in its infancy till the 90s. Significant discoveries were made in the 1980s to scrutinize multichannel data. Principal component analysis, originating from the field of mechanical engineering (Pearson, 1901), was cleverly applied to sorting extracellular recordings of spikes from different origins (Schmidt, 1984) and then applied in automated fashion several years later (Kreiter, Aertsen, & Gerstein, 1989). Some variation upon principal component analysis is the most popular choice for post-processing multi-channel extracellular recordings. Another popular spike sorting methodology based on matching spikes to a mean template was also first described around the same time (Mankin, Grant, & Mayer, 1987), and is still a popular choice for real-time sorting. However, it wasn't till the increase in pace of research during the 90s that those methods were most utilized. Since earlier microelectrode arrays had relatively wide spacing between electrodes ranging from 200µm or higher, analysis could be done on each electrode individually. This increases data value by minimizing redundancy (Carlson & Carin, 2019). This can be applied to tetrode analysis as well, but in a planar matrix configuration there is more crosstalk from overlapping recording fields. Since spikes can potentially be detected at distances of 100µm or more from the neural soma (Buzsáki, 2004; Einevoll, Franke, Hagen, Pouzat, & Harris, 2012; Pettersen & Einevoll, 2008; Segev, Goodhouse, Puchalla, & Berry, 2004), not only are more neurons detected on the same channel they also have higher likelihood of overlapping across channels. In this situation spike sorting, a school of analysis devoted to multichannel electrophysiological recording, is most commonly used for differentiating neural origin. Skipping the post-processing of spike sorting is simpler

and more time efficient, which can be helpful clinically or for cursory evaluation experimentally, but it disregards that the signal per electrode is cumulatively multiple signals of different neural origins. It has been demonstrated recently that manual and automated spike sorting are almost equivalent, and both are superior to unsorted data (Todorova, Sadtler, Batista, Chase, & Ventura, 2014). The inferiority of unsorted data has been shown in both theoretical simulations (Ventura, 2008) as well as more traditional experimental data (Kloosterman, Layton, Chen, & Wilson, 2013; Stark & Abeles, 2007; Ventura, 2008). Very recently an alternative method has been proposed where the clustering portion of spike sorting has been ignored. It was shown that dimensionality reduction alone using primary component analysis was sufficient for neural population dynamics (Trautmann et al., 2019).

In order to separate spikes from background noise, a detection algorithm is first implemented on the raw data to excise small portions of the recording that represent unsorted spikes. Initially spike detection thresholds were fixed (Lewicki, 1998), and based on voltage amplitude set by the experimenter. Since then, other features have been used as threshold criteria such as energy, nonlinear energy, and signed energy, however standard deviation from the baseline noise (sigma) of voltage still seems to be the most dominantly used (Carlson & Carin, 2019; Lewicki, 1998). Detected spikes are clustered based on shape or extracted features, and classified into separate units representing an individual neuron (Quiroga, Nadasdy, & Ben-Shaul, 2004). Detected spikes can be broken down into many waveform features which can be used to extrapolate neural origin such as maximum voltage (peak), minimum voltage (valley), the difference between maximum and minimum voltage (peak-valley), area underneath the waveform, energy, the time to reach peak or valley from beginning of captured waveform, or the time to reach half of the maximum peak or valley, and at it's most basic form simply the voltage

at a specified time slice. Since spike waveforms originating from the same neuron tend to be of very similar shape, the spike feature components can be used to distinguish spikes from different neurons. At it's core this is about dimensionality reduction. A noncontinuous recording is a product of spike detection method on a raw recording. It consists of series of waveform segments that have been excised from the raw recording. Each waveform segment can be reduced to one number based on a variable, also known as a primary component. That variable can be represented by a one dimensional axis, and each waveform can be represented as a specific coordinate along that primary component axis. A single waveform can be considered a distinct point in *n* dimensions, with *n* being the total number of principal components measured. Since early spike sorting mostly relied on human oversight for clustering, two or three components were chosen to be spatially represented for manual definitions of cluster boundaries. Primary components are listed according to variance amongst it's coordinates, the primary components with the highest variance are discarded as noise. The lowest two or three variables are kept, depending on whether clustering will be done on a two-dimensional or three-dimensional primary component analysis feature space.

Clustering algorithms have been used in many fields such as finance, epidemiology, physics, and bioinformatics for unsupervised categorization of data into homogenous groups. Cluster analysis is a machine learning approach to exploratory data mining and grouping. It is not a specific algorithm, but a family of solutions for optimal autonomous categorization. This field has evolved greatly over the past several decades and continues to expand quickly. There is no agreed upon gold standard for spike sorting, which entices new entries into peer reviewed publications on a regular basis. Although early methods of clustering using tetrode data were manually done with the user defined margins (Gray, Maldonado, Wilson, & McNaughton, 1995),

human error must be taken into consideration because of its subjective nature. One of the first implementations of clustering algorithms in electrophysiology was in 1964, well before multichannel systems were implemented, but still utilized field potential recordings in what was termed a 'macroelectrode', since it picked up the summated activity of multiple neurons (Gerstein & Clark, 1964). Although this was one of the first studies using template matching to sort spikes, but it still has great interest to many presently.

The K-Means algorithm is one of the oldest and most popular algorithms for cluster analysis (Forgy, 1965; Lloyd, 1982). However, a great limitation in this method is that it requires the users to set a start position for the clusters and the number of clusters. Each point of data is assigned to its nearest cluster center and then the cluster centers are recalculated based on the points assigned to it. Regrouping toward nearest cluster and recalculating centers is repeated until there is no change. After convergence has been achieved, points that are a user defined ratio of standard deviation from cluster centers are eliminated. The Expectation Maximization (E-M) algorithm is an iterative method that assigns data points based on a user defined number of Gaussian distribution based clusters (Dempster, Laird, & Rubin, 1977). Clustering using E-M can be broadly categorized into two main steps, an expectation step and a maximization step.

Valley Seeking is an iterative nonparametric cluster analysis algorithm (Koontz & Fukunaga, 1972). It is iterative because a portion of the algorithm loops until all points are assigned to a cluster or until the maximum number of set iterations has been met. It is nonparametric because it requires no assumptions about the frequency distribution of the data. Valley seeking begins by making a density estimation by calculating the number of neighbors within a critical distance from each individual point (Yip, Ding, & Chan, 2006). Critical distance can be defined as:

Critical Distance = 0.25 * sigma * Parzen Multiplier

Sigma is a user defined multiple of the standard deviation of all points to a mean. The Parzen Multiplier is another user defined variable representing a criteria for cluster density (Duin, 1976). It shares similarities with Parzen density estimation kernel algorithms (Chen, Hong, & Harris, 2004; Hong, Chen, & Harris, 2008). Then seed points with the highest number of neighboring points are categorized as cluster centers. Any other seed points within critical distance of cluster centers will be included within the cluster, and if another cluster center is within critical distance then the those two clusters will be combined. There are two main reasons why Valley Seeking is exceptional for *in vitro* multichannel data as compared to other clustering algorithms. One, it requires less assumptions. Both K-Means and E-M algorithms require the user to define a preset number of units per channel, while Valley seeking does not. When stereotaxically implanting a tetrode or MEA *in vivo*, one will get a good approximation of the number of units detected per channel after several repeated recordings in the same location. However *in vitro*, the number of units detected by a specific electrode on a different probe will not be related because the network will be different. As a culture evolves over time, the number of units on a specific electrode may also change with time (Fig 8). The second major advantage of Valley Seeking over other clustering methods is the degree of user customization available. Varying sigma allows a user to define the size of a cluster, while varying the Parzen Multiplier allows a user to define the density for clusters. For example, if the signal to noise ratio of a recording is poor then Valley Seeking can be used as an additional filter to remove noise based on waveform shape.

## CHAPTER III: PRELIMINARY STUDIES

Initial studies were done on murine models because of the potential access to a myriad of lines of genetically modified mice available. Due to previous research in the lab, there was specific interest in spinal muscular atrophy (SMA) models based on knockdown of survival motor neuron (SMN) proteins. Also, optogenetic techniques were a burgeoning field in neuroscience so great interest was also directed toward channel rhodopsin models using a ChAT promoter. However, since very few labs in the world are committed to primary culture of lower motor neurons much of the training needed to achieve viable cultures was achieved through trial and error. Although our lab had successfully achieved primary cultures using rats, it had never been done successfully before in our lab using a mouse model. Some of the main difficulties that arose were due to size of mice embryos and the robustness of mouse motor neurons. This was compounded by the lack of onsite animal facility, which limited access to timed pregnant mice required for primary culture from embryos. Since mouse motor neurons are most viable in culture when taken from 12 -13 day old embryos, all experiments would require one month advance planning in order to obtain timed pregnant mice at the appropriate dates. The technique and protocols I inherited also simply did not work.

Murine spinal motor neuron cultures are traditionally harvested from E12.5 to E14.5. A typical timed pregnant mouse can have about 6 to 12 embryos, each of which would take approximately 45 minutes to an hour to dissect. The dissection was extremely difficult because of the small size of the embryos, and I experimented with different dissection techniques, finally settling on ventral approach known as a laminectomy, a common technique used by neurosurgeons in humans. Not only did this allow me to bypass removal of gastrointestinal structures, but removal of the spinal column was not necessary. Having the spinal column remain

*in situ* was advantageous as it allowed anchoring and stabilization for dissection of the spinal cord. Leaving the spinal column and GI organs intact not only decreased processing time and effort, but also increased culture viability as the neurons could be plated more quickly.

Removing the meninges from the fragile, nearly microscopic cord was also quite an ordeal. I was advised to take the meninges off was in the fashion of a sock, however, this was difficult. Meninges has a higher tensile strength at this age than a spinal cord so this would cause the soft cord to break. I then tried to remove the meninges bit by bit, which was both time consuming and caused gouging of the cord. I also tried cutting the cord along a coronal plane, which was highly inaccurate technically. A spinal cord is not straight due to both lumbar and thoracic curvatures, which would cause uneven division between the ventral and dorsal portion. In addition, scalpels normally used for general dissection or surgery had blades that were almost the width of the cord. I solved this by opening the spinal cord dorsally and exposing the central canal. This would allow me to open the spinal cord like a book, with the meninges lying solely on one side like a book cover. I could then peel away the meninges as a sheet. I could then cut the outer left and right portion away, which would consist of the dorsal horn, leaving the central portion which would consist entirely of the ventral horn. I solved the scalpel issue by changing to an ophthalmic scalpel, commonly used in cataract surgeries, which had a micro-feather blade.

At first, cultures appeared dead on plating, so decreasing dissection and processing time became of great concern since dissecting a dozen embryos by myself in one sitting could take up to 10 hours. The protocols provided to me stated storing dissected spinal cords in chilled Hank's Balanced Salt Solution (HBSS) until processing. I later changed this to culture media with little improvement. Hibernate (BrainBits, LLC), a medium that allowed maintenance of neural cells in ambient $CO_2$, while maintaining pH and osmotic balance, improved things somewhat. This

improvement was increased further as Hibernate-E and Hibernate-A derivatives became available, specializing in either embryonic or adult primary neurons. However, cells still did not lookvery healthy when stained with trypan blue for cell counting, and cell counts were low. The original protocol I was provided included a step for centrifugation using a cushion of bovine specific antigen (BSA), which would allow for removal of debris. I removed this step as it was redundant with the Optiprep gradient centrifugation step used to separate the motor neurons from the astrocytes and other cellular component of the spinal cord. In addition, I began doing the dissection with chilled HBSS and doing all centrifugation at 4°C to help preserve viability of the cells. Now the ventral horn motor neurons looked healthy upon staining with trypan blue for cell counting but would be dead within one day of *in vitro* culture. I concluded that the issue must lie in the media.

This began a long expedition to optimize the cell growth media. When one examines the long history of cell culture, investigators have used a wide variety of components to increase viability of their cultures. Growth factors such as glial derived neurotrophic factor (GDNF), brain derived neurotrophic factor (BDNF), B27, and l-glutamine are commonly used but the concentration of these growth factors is not really agreed upon. At this point I stopped using penicillin-streptomycin because of possible toxicity. Although it increased likelihood of contamination, toxicity and cell health was more of a concern. Over the period of a couple years I titrated and optimized levels of the aforementioned growth factors and experimentally investigated the use of others such as ciliary neurotrophic factor (CNTF), insulin like growth factor (IGF), cyclic adenosine monophosphate (cAMP), GlutaMax, N21 media supplement, sodium pyruvate, glucose, fetal bovine serum, horse serum, rabbit serum, as well as a host of others. Not only were each of the growth factors and supplements tested for, but they were tested

in varying concentrations with each other to ascertain possible synergistic effects. All this research quickly became obsolete when I discovered NbActiv4 created by BrainBits, LLC. This media is optimized for cell culture and electrophysiological studies contained three key ingredients that I had never thought to study: creatine, estrogen, and cholesterol.

Two other issues that were occurring concurrently was that the neurons did not tend to anchor and extend axons, which I concluded was due to the substrate used for plating. The protocol in the lab for culture of rat motor neurons used laminin and poly-lysine to coat the plates. However, after plating many of the cells would not anchor and those that did would have little to no axonal extensions. I tried various dilutions of both laminin and poly-lysine and various temperatures and durations of incubation with each coating but nothing worked. A collaborator at A.I. Dupont then suggested that I use poly-l-ornithine and I tried that various concentrations, with varying durations, and with varying temperatures; none of which worked. Although poly-l-ornithine does not require the use of laminin, I added this into the mix. I tried poly-l-ornithine with laminin at varying concentrations, with varying periods of incubation, and with varying temperatures, but still no success. I also tried CELLstart, as well as other substrate samples that I had been given at the Society for Neuroscience conference. All were done at varying temperatures, with varying durations of incubation, with/without laminin. Although things worked to a limited degree, nothing worked very well. I was then introduced to Matrigel by a neighboring professor who had recently joined our department. The results were outstanding compared to others. Not only did the cells anchor very well, but axonal extension was prolific.

With cells anchoring, the next issue that arose was that cells would clump together in balls resembling neurospheres, which could also be described as gastrulation. I changed the dissociation step by triturating the cells via a 1ml micropipette tip as well as chemically

dissociating with trypsin. Efficiency of trituration increased dramatically with the use of a fire polished pipette. Since the efficiency of trypsin decreases dramatically at room temperature I was suggested to use papain, which has the added benefit of being a more gentle chemical dissociate as compared to trypsin, however it ended up being to gentle. I finally landed on TrypLE, which not only had the enzymatic efficiency of trypsin but also was very stable at room temperature over long periods.

I had finally solved many of the technical challenges of embryonic culture with mouse neurons, however, getting pregnant mice with the right timing was still difficult. Around this time I had come across a publication showing postnatal motorneuron cultures (Milligan & Gifondorwa, 2011). Although embryonic tissue has been the traditional source of harvesting cells for most cell types over the history of cell culture. If the right conditions could have such a dramatic effect on my embryonic cell cultures, could those same conditions have a dramatic effect on postnatal cell cultures? Since dissection and processing causes great traumatic injury to cells, perhaps the right conditions could cause those cells to recover and regenerate. The possibility of postnatal cultures has benefits both at the research level of a small institution as well as translational implications medically. Obtaining an accurate date of insemination after mating can be a little difficult. It requires identifying a viscous vaginal plug the following morning after copulation. Identification of a vaginal plug is indicative but not a guarantee of conception. The vaginal plug typically lasts for 8-24, and may have fallen out by the time of checking. I found this method to be highly inaccurate. This was quite a difficult time for me as we had just started an elementary animal room, but had no technician. I was responsible for ordering bedding, food, and supplies for not only our lab but all the labs in our department. I had to maintain food & water for our mice, clean cages by hand, set up matings, and do genotyping.

After those tasks were completed then I could focus on producing cultures, maintaining cultures, and doing recordings. When I could schedule free time then I would focus on immunocytochemistry, developing a ChR lenti-virus vector, or trying to stimulate the cultures pharmacologically, electrically, or optogenetically. If I could develop a postnatal motor neuron model it would be a great reduction on the drain of our resources both financially as well with time. Growing a female mouse to reproductive age would take approximately 2-3 months, and harvesting the embryos would eliminate that female mouse at her prime for our colony. Post-natal motor neuron cultures would have also been a great boon translationally as one of the greatest obstacles to recovery from traumatic spinal cord injury is loss of motor neuron function. If it could be shown that under the correct conditions that lower motor neurons could recover and regenerate, this would be a great advance translationally for recovery from spinal cord injury in patients. On a positive note, the work I had put into optimizing culture techniques for embryonic motor neurons did translate well to culturing postnatal neurons, the cultures appeared to be healthy and morphologically like published motor neurons *in vitro*. However, I ran into the same difficulties as I had with the embryonic cultures in that I found little ChAT expression and spiking activity did not show bursting or synchronized bursting activity.

After approximately 100+ cultures and about 300 recordings, I had more confidence that the actual culturing process was working. Now that the murine motor neurons were anchoring, extending axons, and showing viability over long durations the last piece of the puzzle was firing activity. An additional 50+ cultures and 160+ recordings were done after the culture system was working effectively. The traditionally accepted pattern of firing of primary cultures *in vitro* is a progression from relative silence, to spontaneous firing, to uncoordinated burst firing, to synchronized burst firing. Although I was able to record some neuronal firing from cultures, it

did not follow the typical pattern of firing seen *in vitro*. The motor neurons were progressing to spontaneous firing, but not beyond. Little to no bursting activity was seen across cultures, and no synchronized bursting was seen across channels. I believed that if the neurons could be induced into firing that perhaps something more commonly seen amongst published works could be induced. Our MED64 system could stimulate up to two electrodes simultaneously, however little change was seen with stimulation. Pharmacological stimulation was attempted with serotonin, glutamate, acetylcholine, and high potassium but the result was always inhibition. Since neural cultures are extremely sensitive to temperature, pH, and $CO_2$ changes, this was assumed to be the cause of overall dampening of the network.

An option which was of great interest at the time was optogenetics, as this technique was growing quickly in popularity amongst the field of neuroscience. Optogenetic stimulation would have been quite ideal in that would have allowed stimulation without alterations in the properties of the media. I was also being heavily questioned by colleagues at the time whether these were even motor neurons at all. Since the channelrhodopsin in the mouse line we were examining was expressed after a ChAT promoter, then only cholinergic cells would be stimulated. The ChR chosen had the additional benefit of being an EYFP fusion protein. Since ChAT staining up until this point has yielded unsatisfactory results, I blamed it on poor technique. With a genetically encoded fluorescent marker we could identify cholinergic cells simply by illumination, bypassing the need for antibodies. At first, I relied on the collaborator at A.I. Dupont for a supply of channelrhodopsin (ChR) mice because he was crossbreeding that strain with an SMA knockdown that was being utilized by another collaborator at Johns Hopkins. I was rather confused that the cultures did not show EYFP expression. I tried optical stimulation to no avail. Genotyping didn't seem to confirm that it was ChR positive, but I was assured by the

collaborator that they were ChR positive. Later I discovered that he was having difficulty crossbreeding as well as genotyping. The mice that he was sending me as ChR positive most likely were not ChR at all. We later purchased our own mice directly from Jackson Lab, and the genotyping was working well. EYFP expression on slices was faint but confirmed that there was ChR there. However, when cultured the ChR-EYFP expression disappeared. The mouse line was scrapped, and I proceeded to make a lenti-virus with ChR. Although it would not be selective for cholinergic cells, I could at least do some optogenetic stimulation. Unfortunately, transfection efficiency was extremely low, and little to no stimulation was achieved.

I was now under the impression that the cells I was culturing were not in fact cholinergic, they must have been something else. It was suggested that I move on to the NSC-34 cell line, a mouse motor neuron neuroblastoma hybridoma. I also was able to obtain a SMN knockdown version of this cell line from University of Indiana. However, after almost 100 cultures and over 700 recording the firing pattern did not represent anything seen typically in neurons in primary culture or *in vivo*. Spontaneous firing was not constant through the recording, bursting was highly concentrated around certain time points, and there was little synchrony across channels. In addition, around this time a paper had been published that showed that these cells were an unsuitable model for glutamate-mediated excitotoxicity (Mavel et al., 2016), so this project was also scrapped. It was at this time that I began to think that I might be able to push primary spinal cultures into being cholinergic by coculturing them with myocytes.

I decided to switch to chick spinal cord cultures for several reasons. Chick neurons appear to be hardier *in vitro* than murine neurons. They have a long history in neuroscience as an accepted culture system. The gestation time of chickens is approximately the same as mice, 21 days, so developmental parallels could easily be made between the two models. The size of

embryonic chicks at the same development time point were much larger, and thus much easier to dissect and process. One or two embryonic spinal cords could easily be dissected in one sitting, as opposed to being forced into dissecting a full litter of mouse pups. Because of decreased cost, spinal cords could be dissected daily if needed.

## CHAPTER IV: MATERIALS & METHODS

### *4.1. Multielectrode Array*

In order to investigate the network electrophysiology of primary cultured neurons, we used the MED64 Basic microelectrode array system (Alpha Med Scientific) with 64 channels and heated stage. The probes (MED-P210A) had 10 mm chamber depth, used a standard 8x8 array with 20x20 μm electrodes and a spacing of 100 μm. Recordings were done for 5 minutes. Input range was set for 25mV, while low pass filter was set at 10 Hz and high pass filter set at 10,000 Hz.

### *4.2. Cell Isolation and Plating*

Embryos were removed from E12 chicken eggs and decapitated. The dissection process was done in chilled HBSS (Gibco, Gaithersburg). The spinal column was removed from the rest of the body and moved to another dish for further dissection. A dorsal laminectomy was performed with #5 forceps, while chilled media was replaced as necessary to compensate for cloudiness from tissue debris. Once the spinal canal was fully exposed, the spinal cord was gently lifted from the column while detaching dorsal root ganglions from beneath. The lumbar and thoracic curvatures were carefully noted for ventral/dorsal discrimination of the spinal cord. A straight incision was made along the dorsal length of the meninges. The lateral portions of the ventral horn were then opened, so that the width of the cord is almost a flat plane. The spinal cord was then placed on the bottom of the dish with the meninges facing up. The meninges was carefully teased away from the caudal portion so that smooth glossy surface of the spinal cord was exposed. The spinal cord was then pinned to the dish with one of the forceps, while the other forceps pulled away the meninges in one clean stroke. Any meningeal remnants were then

removed after inspection. Using a 45° Micro Feather ophthalmic scalpel, the lateral portions of the cord were cut away. Approximately ¼ of the width were removed bilaterally, leaving a central portion consisting of approximately ½ of the total original width.

The ventral horn was trypsinized in TrypLE (Gibco, Gaithersburg) for 5 minutes at 37°C. After washing three times in cold HBSS, it was suspended in cold NbActiv4 (BrainBits, Springfield) for titration by fire polished pipette. A density gradient was created with the ventral horn suspension layered over a chilled 6.8% OptiPrep/NbActiv4 solution and spun at 500 g for 20 min at 4°C. The interface layer, which is primarily neurons, was removed and diluted with 3ml of NbActiv4 and spun at 300g for 10 min in 4° C. The supernatant was removed and resuspended in 1 ml of cold NbActiv4 before plating 200 µl per probe.

For primary astrocyte cultures, embryos were harvested from E10 – E12 chicken eggs and the dissection process proceeded in the same fashion as ventral horn neurons up until after the meninges was removed (Taylor, Robinson, & Milligan, 2007). The same trypsinization, triple wash, and titration process used for the ventral horns was done again, but no OptiPrep density gradient is used. The cells were plated onto large TPP culture dishes with additional chilled NbActiv4. The cells were grown at 37°C in 5% CO2 and half of the media was replaced every 2-3 days. When at 50-75% confluence, the cells were passaged to another plate or plated on a probe for coculturing.

For primary myocyte cultures, embryos were collected from E12 chicken eggs, decapitated and the medial adductor muscles were harvested (Martinello & Patruno, 2008). The muscle was torn into small pieces with forceps for increased trypsinization surface area. The same trypsinization, triple wash, and titration process used in astrocytes was used except the resulting suspension was filtered through a 100 µm cell strainer. The filtered suspension was

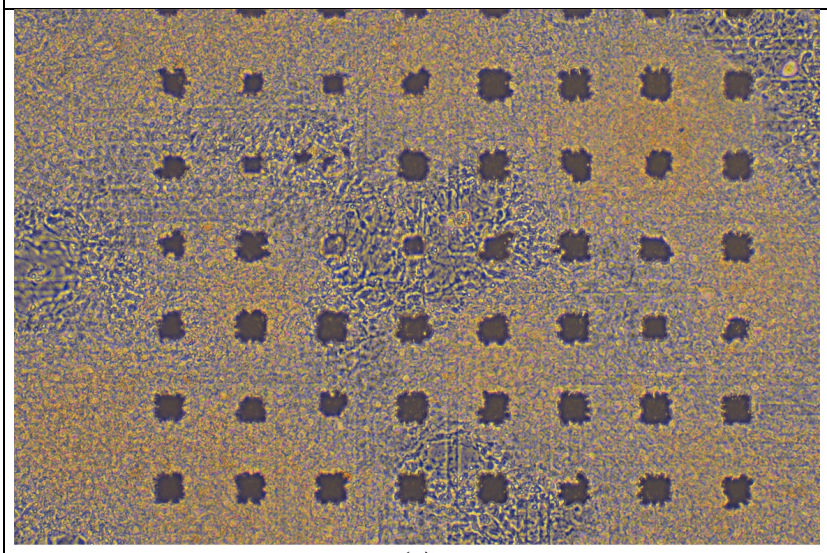

(a)

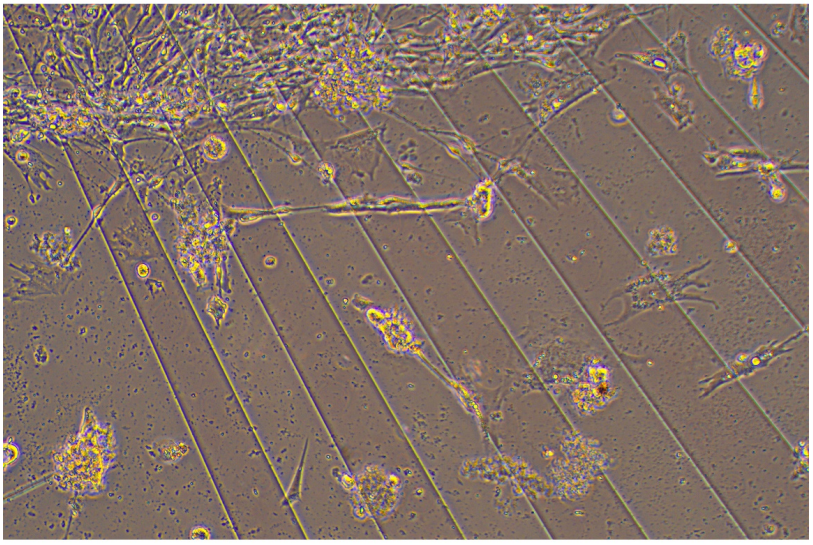

(b)

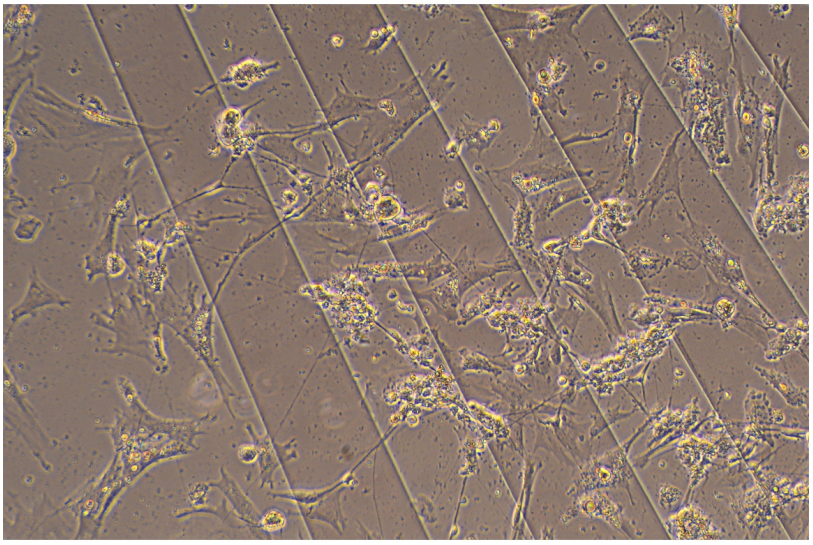

(c)

**Figure 6.** MED64 initial coculture plating density. (a) High density seeding of ventral horn neuron two days after plating. Cell bodies and neurite outgrowths can be visualized toward the center of the field, while much of the visible surface is covered by cell debris. Cell debris will slough off over a week after a few media changes. (b) Further out from the periphery of the electrodes, ventral horn neurons are shown in the lower left portion of the photograph, located closest to the electrodes (not shown). (c) Toward the outmost edge of the probe we see striated muscle cells. Over time the myocytes or astrocytes plated in the periphery will grow toward the ventral horn neurons over the electrodes in the center of the probe.

Approximately 50% of the media was changed every 2-3 days, and when 50-75% confluence was achieved the cells were passaged to another plate or plated on a probe for coculturing.

In order to plate the ventral horn cells, Matrigel was diluted to 25% using NbActiv4 to act as a substrate for culture. A drop was placed over the electrodes, any excess withdrawn, leaving a thin residue, and the probe was placed in an incubator for 3-6 hours, before plating cells, a 8mm diameter cloning ring was centered over the electrodes of the probe. Ventral horn neurons were plated into the center of the cloning ring. For cocultures, astrocytes or myocytes were plated from the outer wall of the cloning ring to the inner wall of the probe (Fig. 6). Around twelve hours after plating, warmed NbActiv4 was added to the perimeter outside of the cloning ring to bring the level to about ¾ of the height of the probe, and the cloning ring was removed. Media was changed every 2-4 days when the phenol red began to change color.

*4.3. Analysis*

Raw output files from the MED64 Mobius acquisition system were imported into NeuroExplorer (Nex Technologies, Colorado Springs) and then imported into Offline Sorter for processing. Any artifacts closer than 50 μsecs and appearing on 75% of the channels were eliminated, and waveforms were then detected at a threshold of -4.5σ from the noise. The detected waveforms were sorted into associated spike template groups per channel using a Valley Seeking algorithm and principal component analysis on a 3D feature space. Under the Valley Seek we scanned Parzen multipliers, which influences how clustering proceeds, from 0.5 to 1.5 with a 0.2 step for each channel. Sorting quality statistic for each multiplier were calculated and the most favorable multiplier chosen56. Outliers more than two standard deviations from the cluster centers were removed. The final sorted file was then exported back into NeuroExplorer for Poisson Surprise burst analysis with a minimum surprise parameter of 3

and then exported into a text file with the results (Gullo, Maffezzoli, Dossi, & Wanke, 2009). We used custom code written in Origin C for OriginPro Graphing & Analysis to determine bursts that overlap temporally over different channels. This can be defined as network bursts and is used by us as an indication of network synchronization. If a burst occurs on six or more channels within the same temporal space, it was defined as a network burst.

Text files of per-waveform, per-unit, and per-channel data with the timestamp, spike amplitudes, and spike energy were saved and investigated using Origin Graphing & Analysis software package (OriginLab, Northampton). Since we were examining change over time, orders of magnitude are more important than linear change. In order to more closely examine the data in a ratiometric fashion we implemented a logarithmic transformation on our final data. This had the additional effect of bringing things closer to a normal distribution, allowing Grubs' Test for Outliers at a significance level of 0.05 to be used to remove abnormal recordings that appeared to outliers. There were a total of 109 control culture recordings, 75 muscle co-culture recordings, and 74 astrocyte co-culture recordings. Of those there were outliers in 2 control culture recordings, 3 muscle coculture recordings, and 4 astrocyte coculture recordings. If an outlier was discovered for any one variable, then the entire recording was discarded.

*4.4. Data Availability*

Both raw recording files and analysis are available as an open access dataset (DOI: https://doi.org/10.21227/vysa-yg14) via IEEEDataPort under creative commons license.

# CHAPTER V: RESULTS

## *5.1. Analysis*

Ventral horn neurons were dissociated from embryonic chicks and were plated over the electrodes. In coculture treatments those neurons were surrounded by either chick spinal astrocytes or chick striated muscle, covering the remainder of the probe surface. Raw recordings, as seen on the left column of Figure 15, were processed for spike detection and sorting based on waveform shape, the results of which can be seen on the right column of Figure 15. Spike sorting is the process of organizing extracellular electrophysiological data into interpretable elements. Waveforms originating from the same neuron will have similar shapes. The detected waveforms are then grouped using principal component analysis (PCA), which extracts characteristic features from each waveform on a channel and groups them into categorical units. Each unit is considered to be of single neuron origin. Waveforms are detected by examining spikes that are further than a threshold of 4.5σ from the noise recorded on each electrode (Gagnon-Turcotte & Gosselin, 2015; Rizk & Wolf, 2009; Watkins, Santhanam, Shenoy, & Harrison, 2004). We used a Valley Seeking algorithm in a 3D feature space (C. Zhang, Zhang, Zhang, & Li, 2007), with 0.2 steps. The step that created the best 3D unit clusters defined by Multivariate Analysis of Variance (MANOVA) and p-value is taken as the final sorting.

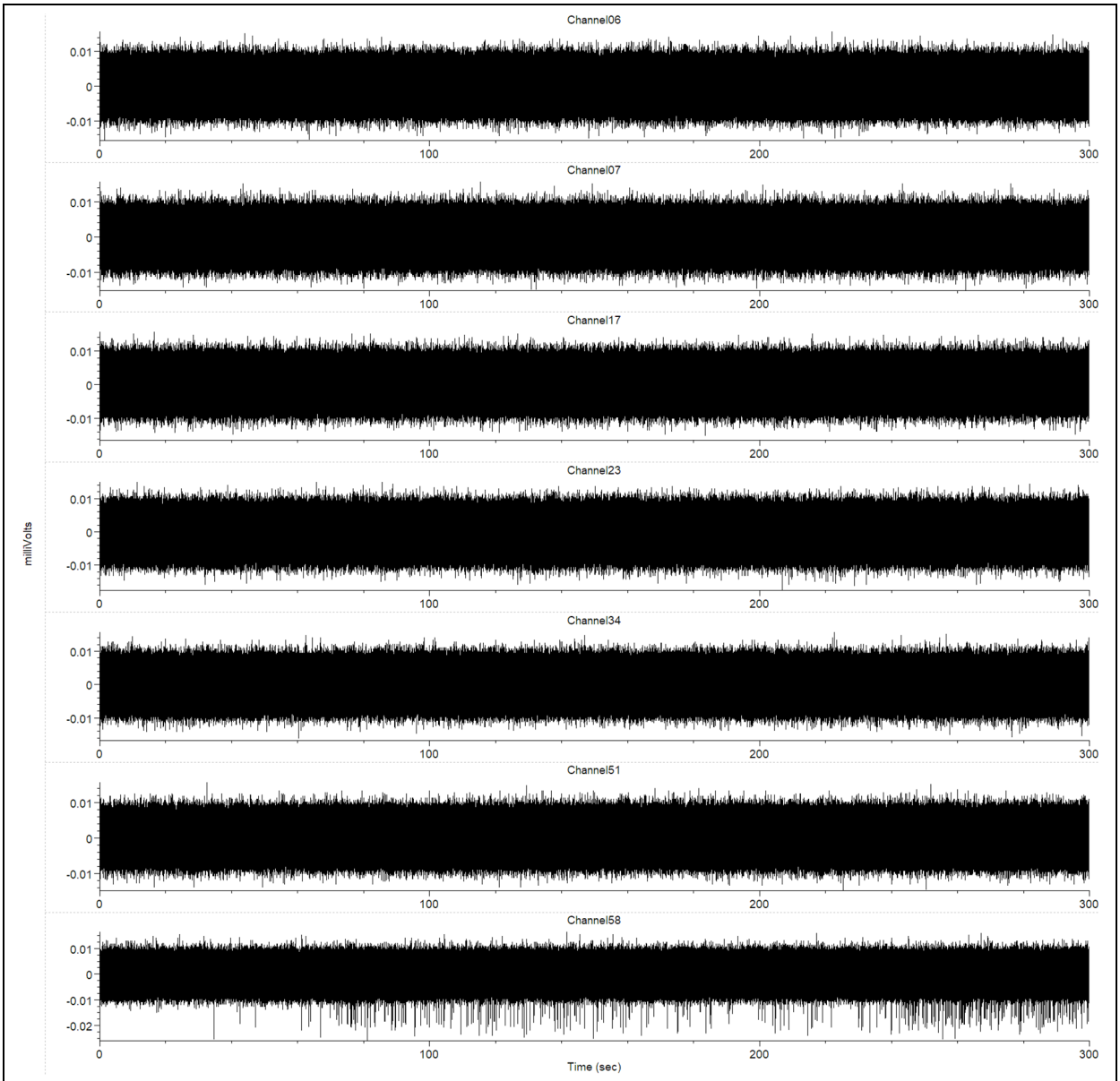


**Figure 7.** Astrocyte coculture 2 DIV. Representational trace of an astrocyte and motor neuron coculture after 2 days *in vitro*.

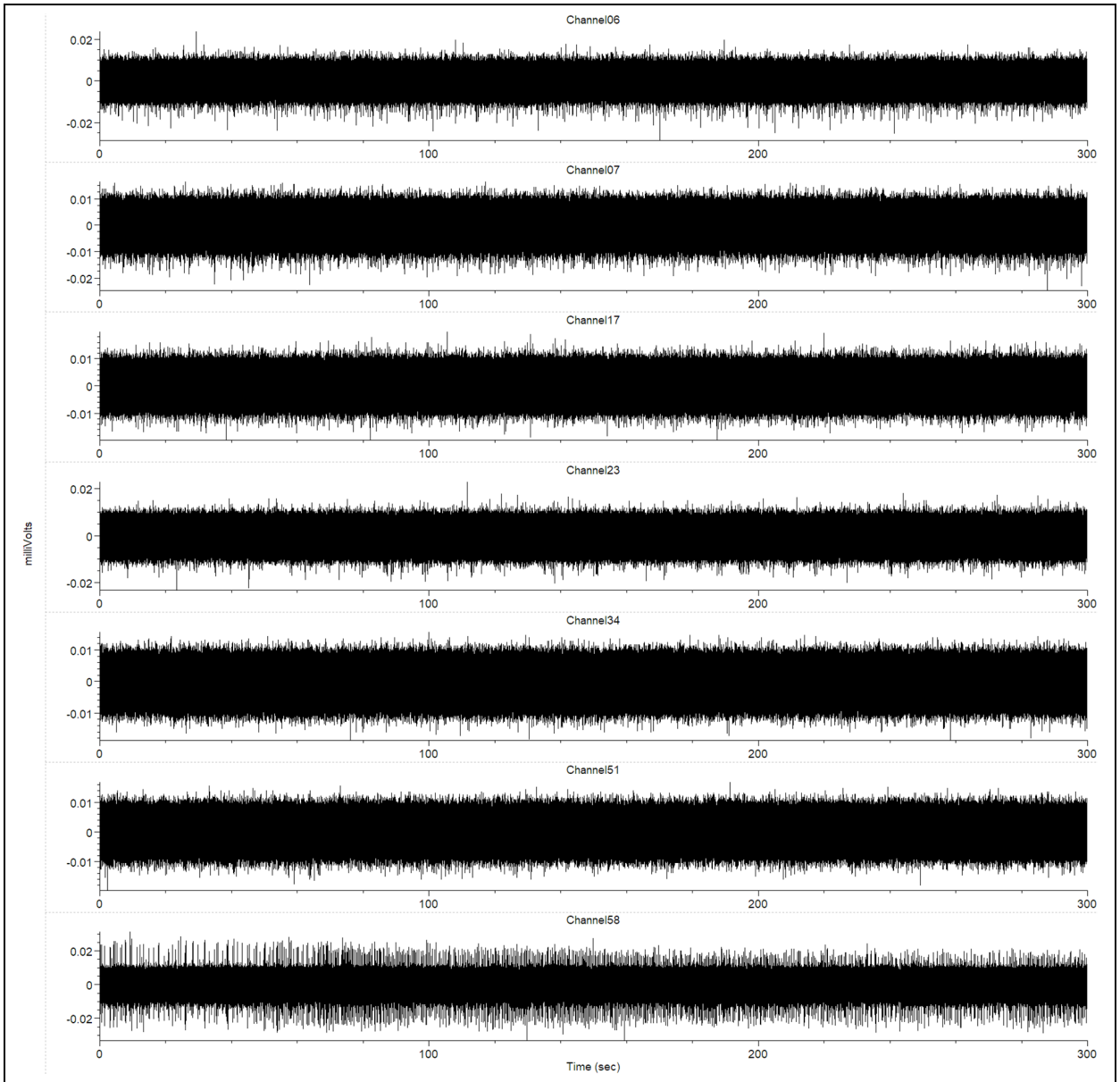


**Figure 8.** Astrocyte coculture 5 DIV. Representational trace of an astrocyte and motor neuron coculture after 5 days *in vitro*. This recording was taken from the same culture as Figure 20.

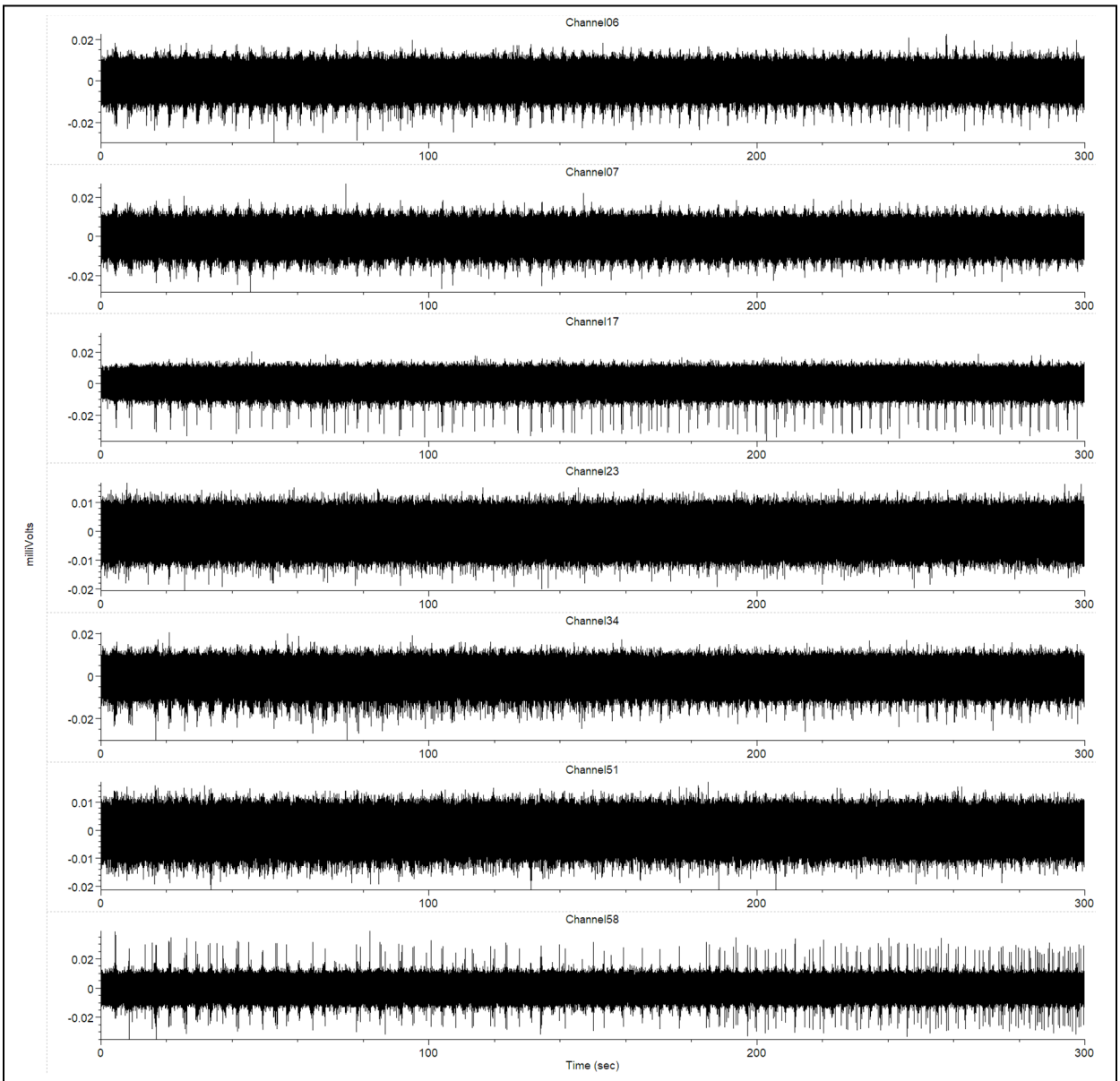


**Figure 9.** Astrocyte coculture 7 DIV. Representational trace of an astrocyte and motor neuron coculture after 7 days *in vitro*. This recording was taken from the same culture as Figure 20 & 21.

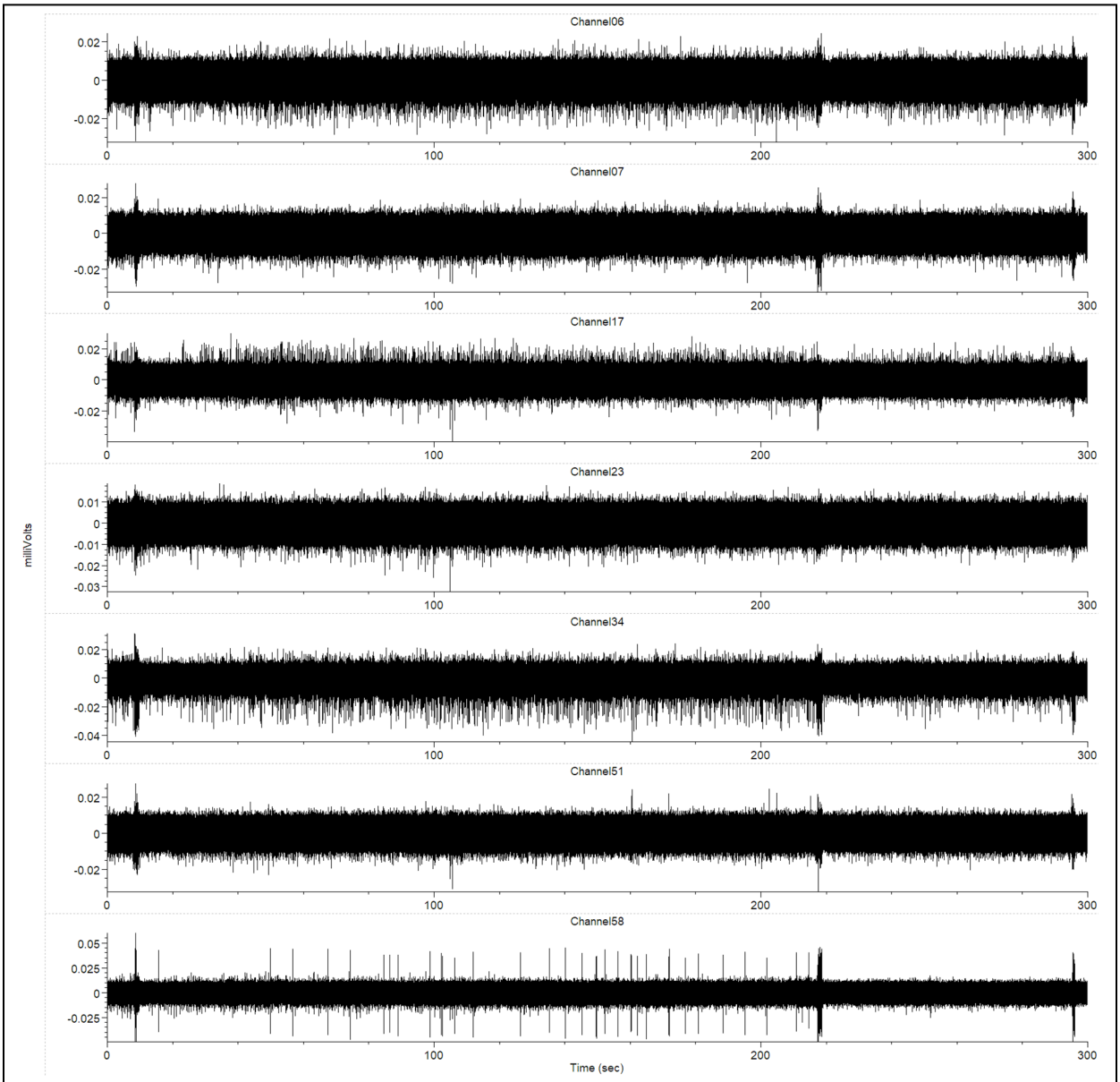


**Figure 10.** Astrocyte coculture 9 DIV. Representational trace of an astrocyte and motor neuron coculture after 9 days *in vitro*. This recording was taken from the same culture as Figure 20-22.

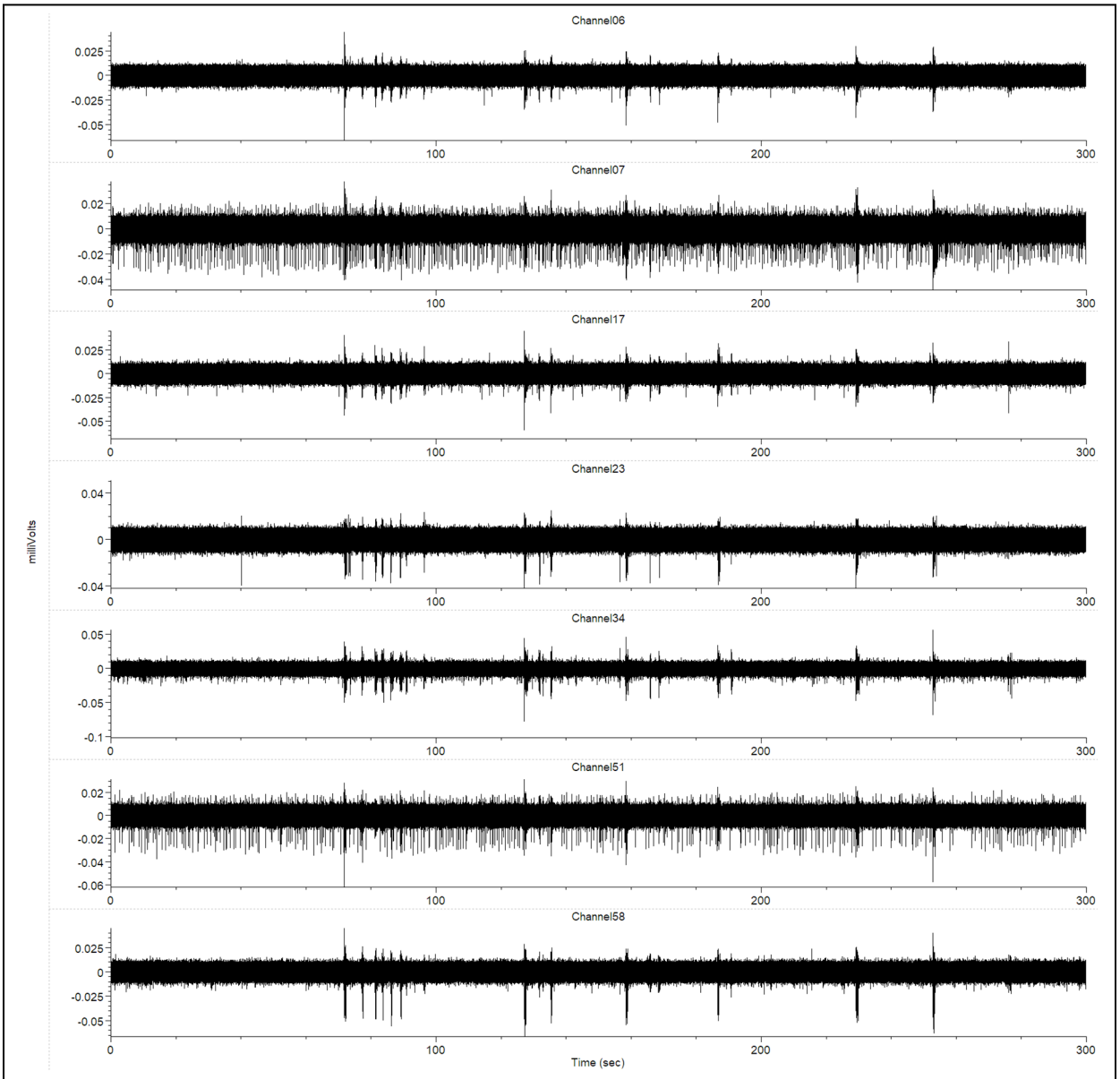


**Figure 11.** Astrocyte coculture 12 DIV. Representational trace of an astrocyte and motor neuron coculture after 12 days *in vitro*. This recording was taken from the same culture as Figure 20-23.

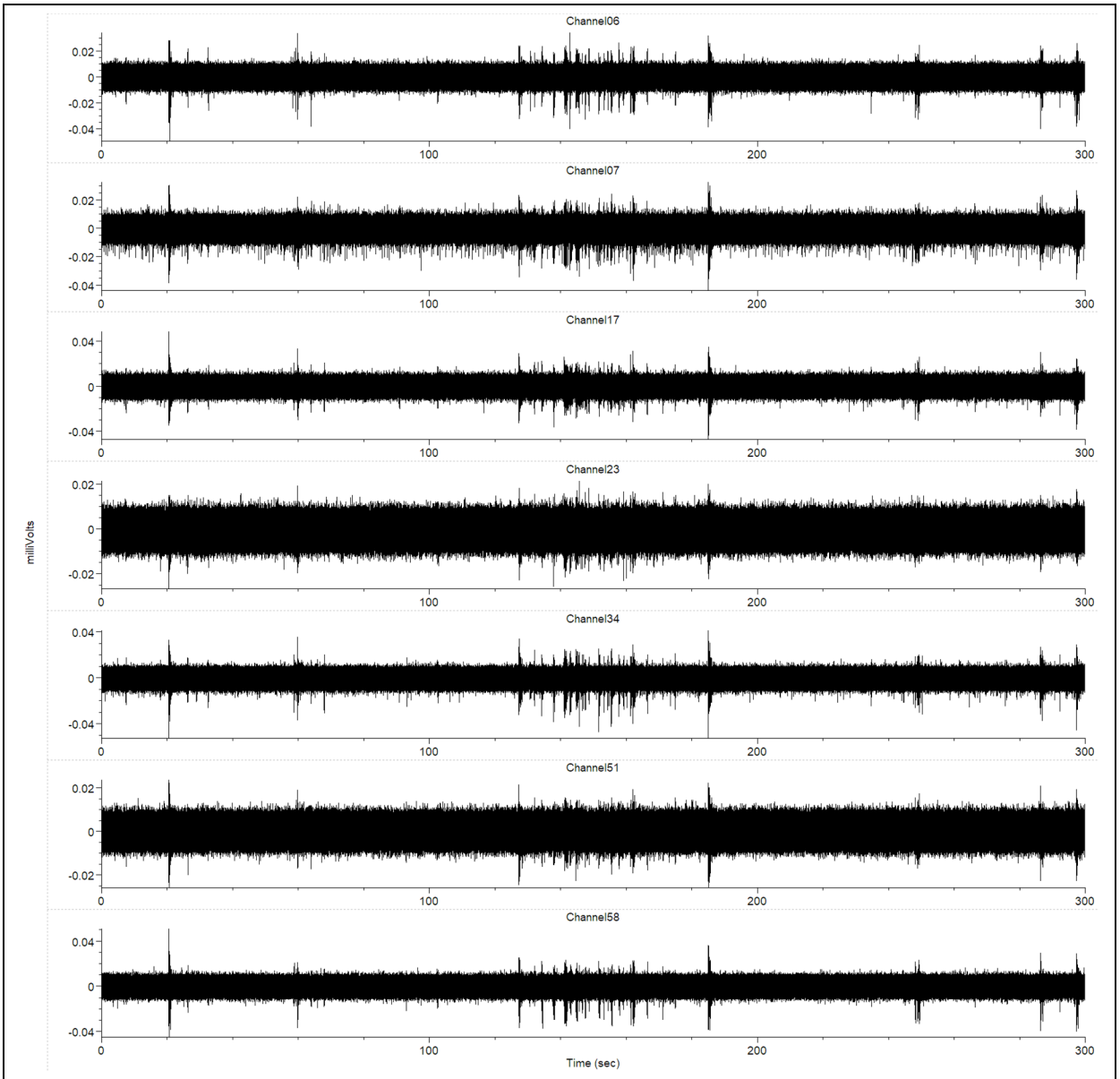


**Figure 12.** Astrocyte coculture 14 DIV. Representational trace of an astrocyte and motor neuron coculture after 14 days *in vitro*. This recording was taken from the same culture as Figure 20-24.

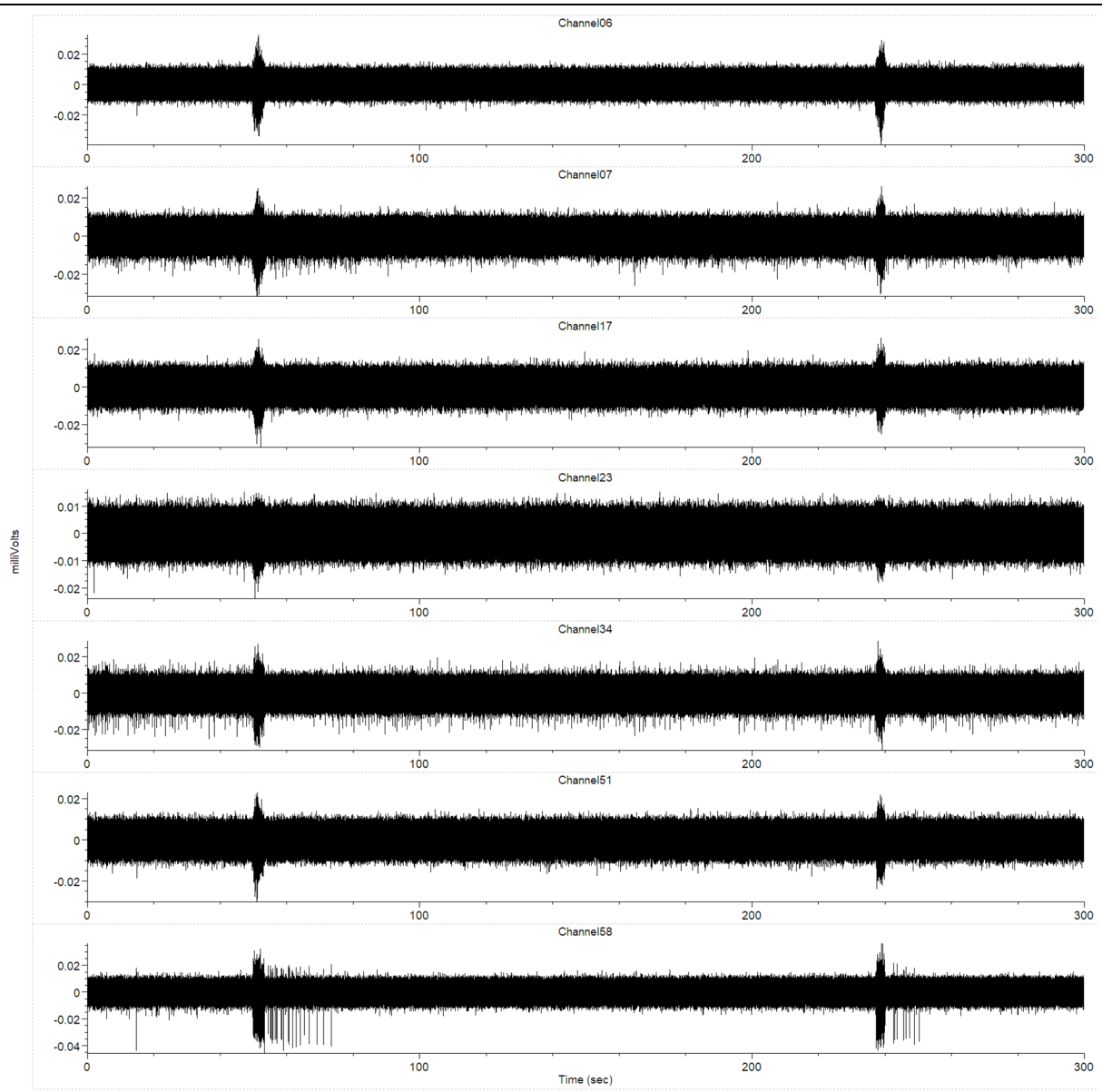


**Figure 13.** Astrocyte coculture 16 DIV. Representational trace of an astrocyte and motor neuron coculture after 16 days *in vitro*. This recording was taken from the same culture as Figure 20-25.

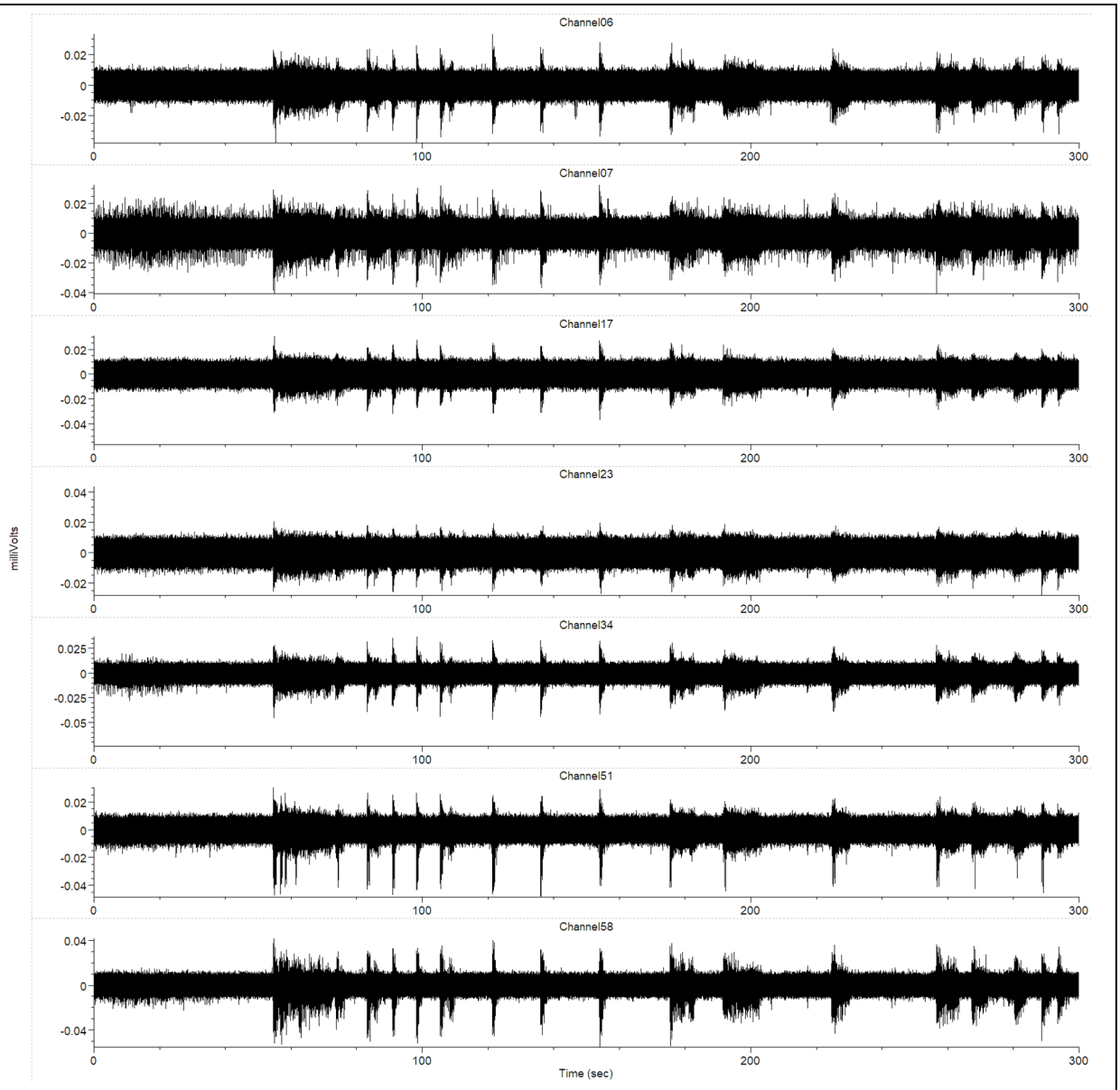


**Figure 14.** Astrocyte coculture 26 DIV. Representational trace of an astrocyte and motor neuron coculture after 26 days *in vitro*. This recording was taken from the same culture as Figure 20-26.

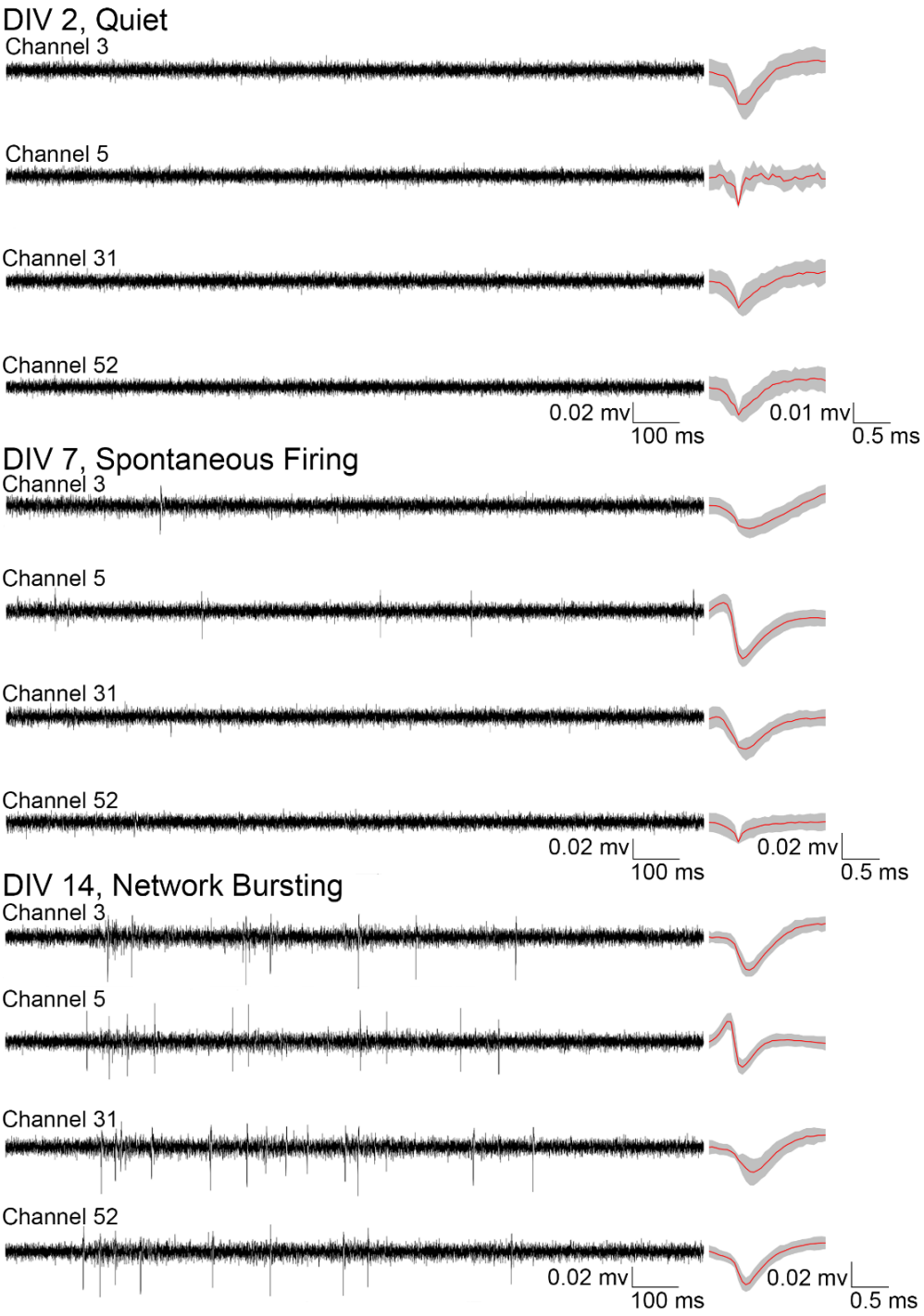


**Figure 15.** Evolutions of spontaneous firing and extracted waveforms. Raw traces of the same channels on the same culture (astrocyte coculture) over the same time period of recording (141-142.5s) on days in vitro 2,7, and 14. On day 2 there is no apparent spiking, while there is distinct spiking on channels 3 and 7 on day 7. On day 14 there is spiking in a train of bursts with temporal synchronization across channels. The right column portrays dominant waveform per channel. The red trace represents the mean of the sorted waveforms for that unit, while the grey area represent waveforms up to two standard deviations from the mean.

*5.2. Spike Characteristics*

All culture preparations start with similar number of total units initially after plating. Two-way ANOVA analysis showed significant ($p<0.05$) differences between cultures with different treatments, between days in vitro, and with culture/DIV interaction (Fig. 16). Since sorted units are assumed to be of single neuron origin, changes in unit count correlate with changes in the number of active nodes of a network. This is an important metric in measuring how the network remodels over time. A logarithmic scale was used to reduce outliers while bringing the data closer to a normal distribution. A logarithmic transformation was not only necessary to fulfill required conditions for statistical analysis, but also made patterns in trends more visible. Both ventral horn cultures and myocyte cocultures showed an increase in total units, log(∑Units), recorded over a 40 day period, but myocytes showed a 57% increase in slope of the line of fit as compared with controls (Fig. 16). Astrocytes showed a rapid decrease in the number of units recorded over time.

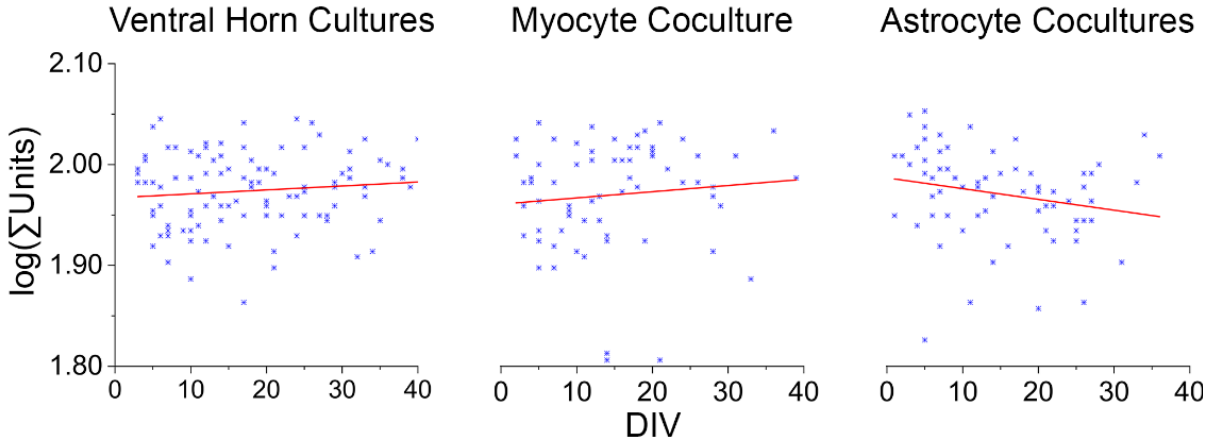


**Figure 16.** Total sorted units. Total number of sorted units recorded over various preparations. Each point represents the total number template units per channels, summed across all channels, and plotted versus day in vitro. Using Two-Way ANOVA, significant differences at $p<0.05$ were found between culture conditions, DIV, and culture conditions/DIV interactions. Spike properties. Ventral horn cultures: 10 cultures, 107 recordings; Myocyte cocultures: 9 cultures, 72 recordings; Astrocyte cocultures: 7 cultures,

The total number of detected spikes, log(∑Spikes), after sorting showed significant differences ($p<0.05$) among culture conditions, between DIV, and with culture/DIV interaction. Detecting spikes gives the most basic metric for evaluating spiking activity of a neural network. There was almost no change over time in the total number of spikes for ventral horn cultures. Myocyte cocultures seemed to show a decrease in spikes over time, although this may be deceiving as there are fewer data points for older recordings (Fig. 17). Astrocytes show a definitive increase in spikes over time and are the most tightly clustered around the line of fit.

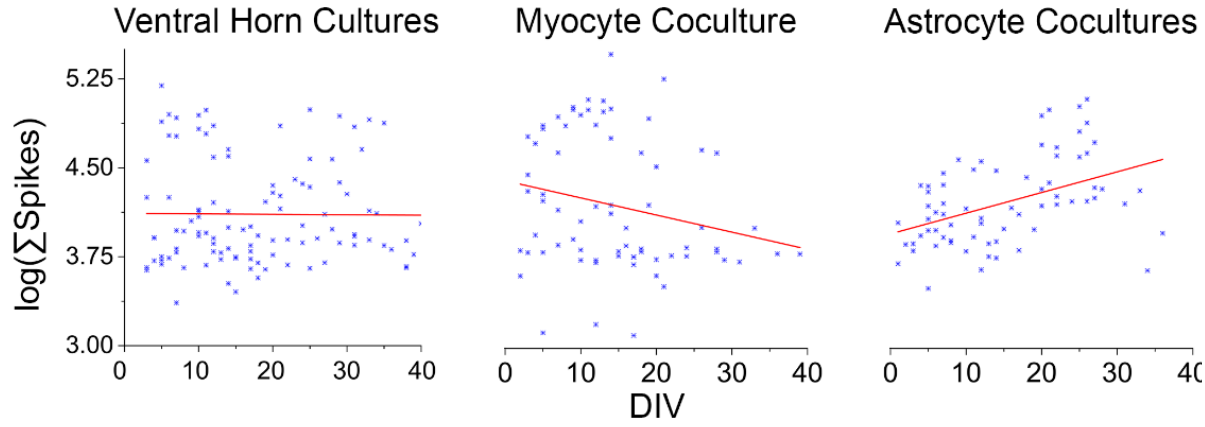


**Figure 17.** Total Spikes. Total number of detected spikes after sorting. Each point represents the total number template units per channels, summed across all channels and plotted versus day in vitro. Using Two-Way ANOVA, significant differences at $p<0.05$ were found between culture conditions, DIV, and culture conditions/DIV interactions. Spike properties. Ventral horn cultures: 10 cultures, 107 recordings; Myocyte cocultures: 9 cultures, 72 recordings; Astrocyte cocultures: 7 cultures, 70 recordings.

The average amplitude, log(Amplitude), of detected spikes after sorting showed significant ($p<0.05$) differences amongst culture types, but not across DIV or culture/DIV interaction. Bonferroni post-hoc analysis showed a significant difference between ventral horn & myocyte cocultures as well as between myocyte cocultures & astrocyte cocultures. Myocyte cocultures were significantly different than ventral horn cultures and astrocyte cocultures in that the average spike amplitudes tended to decrease over time in culture (Fig. 18). For astrocyte

cocultures and ventral horn cultures the average spike amplitudes tended to increase over time. Toward the end of the recording period the distribution of unit amplitudes in the myocytes trends lower than the astrocyte cocultures and ventral horn cultures, even at the beginning of the cultures. Potential factors that might change amplitude in extracellular recordings are changes in the distance of the neuron soma from the electrode, changes in the size and shape of the somas or distribution of smaller and larger neurons, and changes in the frequency of temporally overlapping units on one channel (Chelaru & Jog, 2005; Engel & Hanisch, 2014; F. Mechler, Victor, Ohiorhenuan, Schmid, & Hu, 2011; Ferenc Mechler & Victor, 2012; Pettersen & Einevoll, 2008; Somogyvári, Cserpán, Ulbert, & Érdi, 2012; Swindale & Spacek, 2015).

The energy of a spike is similar, but not the same, as energy in other scientific contexts. It represents the magnitude of voltage required to create a recorded deflection on an electrode during a period of time, which is represented by volt$^2$·seconds. If we were to take into

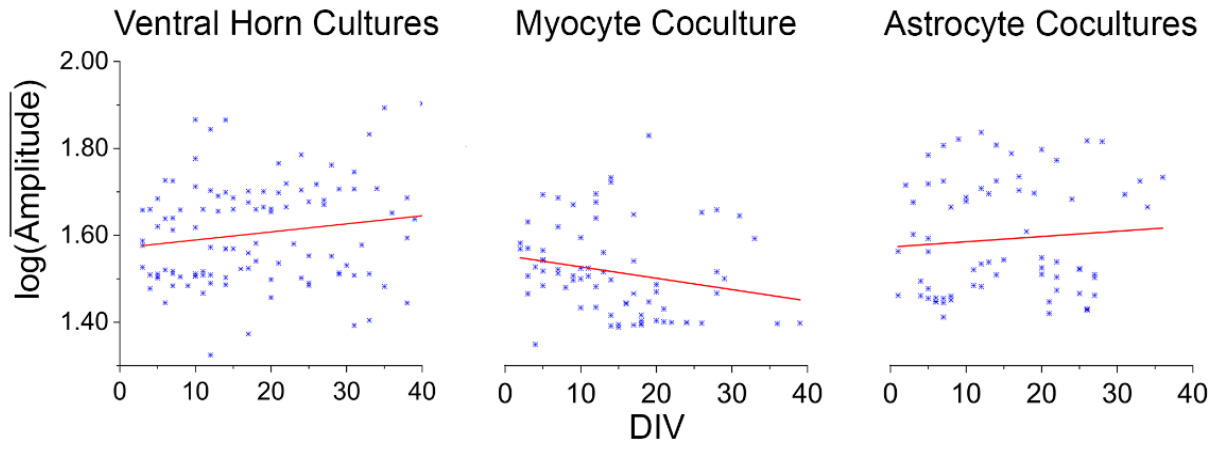


**Figure 18.** Average spike amplitude. Mean amplitude of detected spikes. Each point represents the average amplitude of all sorted spikes from all channels plotted versus days in vitro. Using Two-Way ANOVA, significant differences at $p<0.05$ were found between culture. Bonferroni post hoc analysis at $p<0.05$ showed significant differences between ventral horn cultures and myocyte cocultures as well as myocyte cocultures and astrocyte cocultures. Spike properties. Ventral horn cultures: 10 cultures, 107 recordings; Myocyte cocultures: 9 cultures, 72 recordings; Astrocyte cocultures: 7 cultures, 70 recordings.

consideration the impedance of the electrodes then we would land at a more traditional definition of power.

$$\frac{signal\ energy}{impedance} = \frac{V^2(t)}{ohms} = Power = I(t) \cdot V(t) = \frac{V^{2(t)}}{R}$$

Since spikes can come in all manner of sizes and shapes, the energy of a waveform is a more accurate representation of how much work that neuron did to produce a recorded deflection from baseline. Energy in this context can be defined as volt$^2$·seconds. At time point *i* it is derived by the following equation.

$$Energy(i) = (\frac{1}{width})\sum v(j)v(j)$$

Energy in this context factors in both spike amplitude as well as spike width. It has been shown to be an excellent metric for use in detection of overlapping spikes (Franke, Natora, Boucsein,

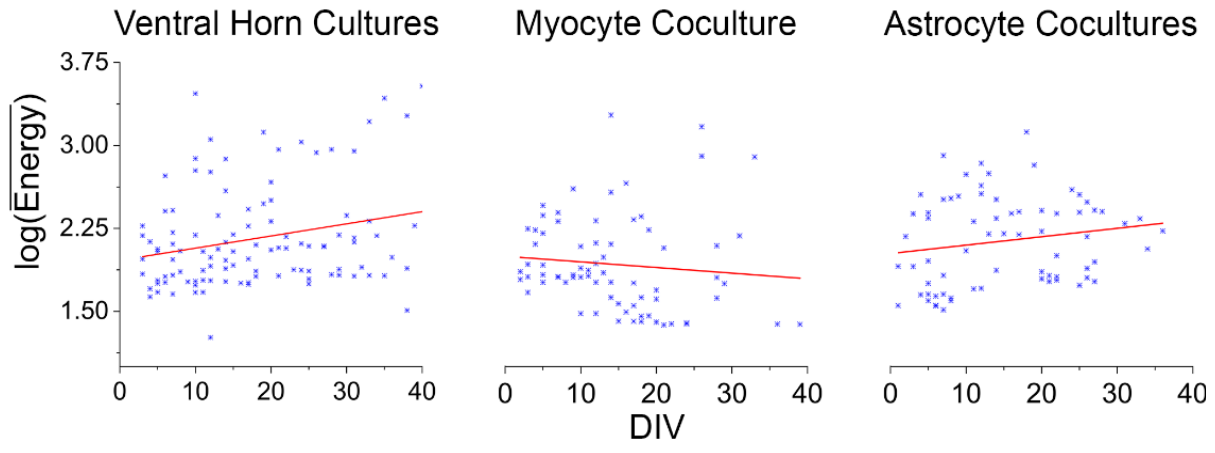


**Figure 19.** Average spike energy. Average energy of detected spikes. Each point represents the average energy of all sorted waveforms during a recording plotted versus days in vitro. Using Two-Way ANOVA, significant differences at $p<0.05$ were found for DIV. Bonferroni post-hoc analysis at $p<0.05$ showed significant differences between control and myocyte cocultures as well as between myocyte cocultures and astrocyte cocultures. Spike properties. Ventral horn cultures: 10 cultures, 107 recordings; Myocyte cocultures: 9 cultures, 72 recordings; Astrocyte cocultures: 7 cultures, 70 recordings.

Munk, & Obermayer, 2010) as well spike sorting under conditions of low signal to noise ratios (K. H. Kim & Kim, 2000). Waveform energy was specifically looked at here because of the low amplitude of firing in myocyte cocultures. While a typical action potential duration in neurons is less than 1 ms, in muscle it is typically 2-5 ms. Since the decrease over time in amplitude of spikes among myocyte cocultures approximates the decrease in energy over that same time span we can conclude that the electrophysiological characteristics seen here are of neural origin.

The mean energy per detected waveforms after sorting showed significant ($p<0.05$) differences amongst DIV and on post-hoc analysis between ventral horn cultures & myocyte cocultures as well as between the astrocyte cocultures and the myocyte cocultures (Fig. 19). All culture conditions initially started around the same point. Over time however, myocyte coculture show a decrease in average spike energy over time while ventral horn cultures and astrocyte cocultures show an increase in waveform mean energy. Significant differences were found across DIV, but not between culture preparations or culture/DIV interactions. However, there is a

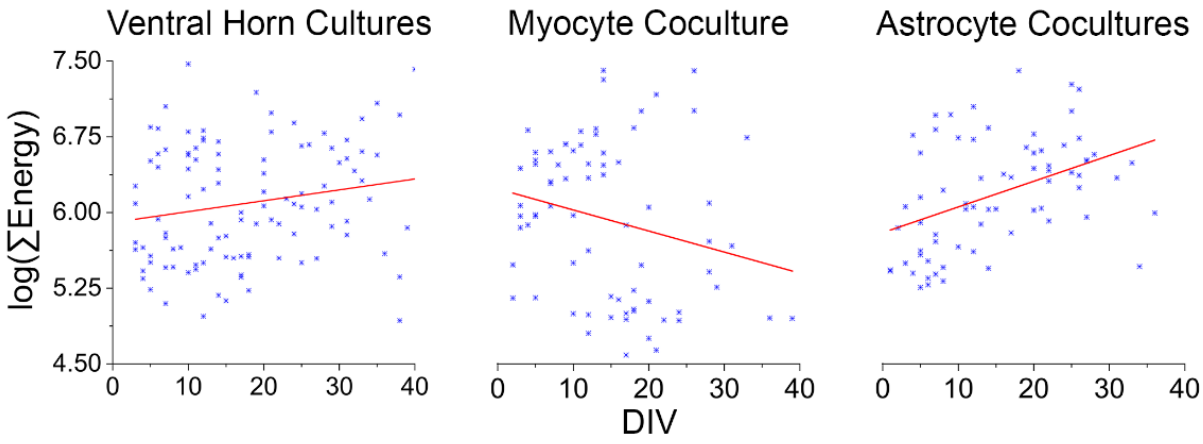


**Figure 20.** Total spike energy. The sum energy of all detected spikes over a 5 minute recording. Each point represents the sum total of all the energy from every sorted waveform in the recording plotted versus time in vitro. Using Two-Way ANOVA, significant differences at $p<0.05$ were found between culture conditions, DIV, and with culture conditions/DIV interactions. Spike properties. Ventral horn cultures: 10 cultures, 107 recordings; Myocyte cocultures: 9 cultures, 72 recordings; Astrocyte cocultures: 7 cultures,

visible upward trend in waveform energy in both ventral horn cultures and astrocyte cocultures, while myocyte cocultures decreased over time.

Reflecting the contribution of changes in the number of units and spikes, and spike amplitudes, the total energy from all detected waveforms during each five-minute recording showed significant differences ($p<0.05$) between culture types, DIV, and culture type/DIV interaction (Fig. 20). Although all culture types start initially around the same level, the total spike energy for astrocytes cocultures increased rapidly, while the total spike energy of myocyte cocultures decreased almost as rapidly. Ventral horn control cultures also increased over time, but only at about half the rate of change as astrocyte cocultures.

*5.3. Burst Characteristics*

Burst firing is defined as a period of high frequency spiking followed by a silent phase. Bursts convey important data in regards to information processing and play a role in synaptic plasticity (Lisman, 1997). Bursts are diverse in characteristics and informationally rich, allowing them to convey more than a single spike (Wagenaar, Pine, & Potter, 2006).

Burst detection was done through the Poisson Surprise method(Legendy & Salcman, 1985). This classic method essentially determines how improbable a burst is as a chance occurrence. The probability, P, takes into consideration the count of n spikes and average spike rate, r, over time interval T. The surprise value is then simply calculated as S = -logP.

$$P = e^{-rT} \sum_{i=n}^{\infty} (rT)^i / i!$$

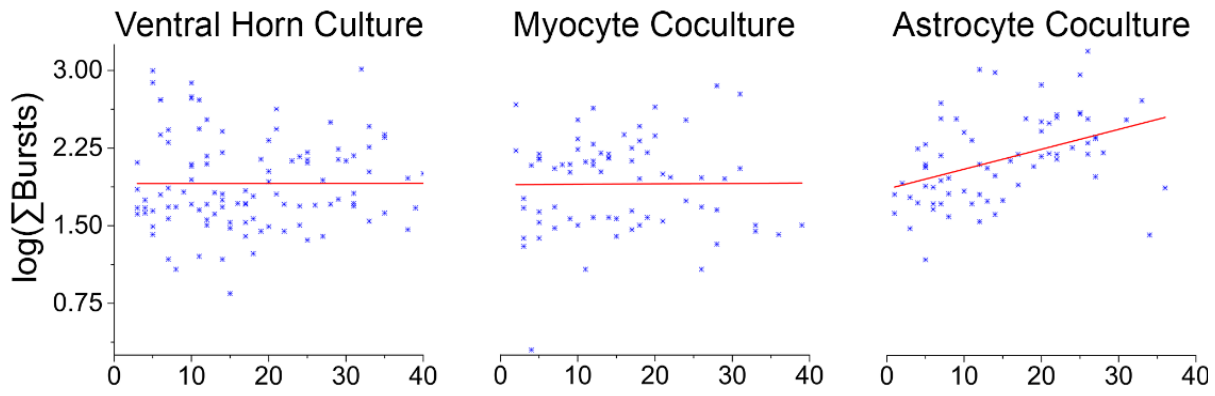


**Figure 21.** Total bursts. The total number of burst detected during a five minute recording. Each point represents the total number of bursts detected in all electrodes in that recording. Using Two-Way ANOVA, significant differences at $p<0.05$ were found between culture conditions. Burst Properties. Ventral horn cultures: 10 cultures, 107 recordings; Myocyte cocultures: 9 cultures, 72 recordings; Astrocyte cocultures: 7 cultures, 70 recordings.

In our recordings, the total number of bursts detected per five-minute recording showed significant ($p<0.05$) differences between culture preparations. All culture models started at approximately the same range and increased with time (Fig. 21). Ventral horn muscle cocultures showed almost no change in burst numbers over DIV, while astrocytes cocultures showed a significant increase in than the total number of bursts. The increase in the ability of astrocyte

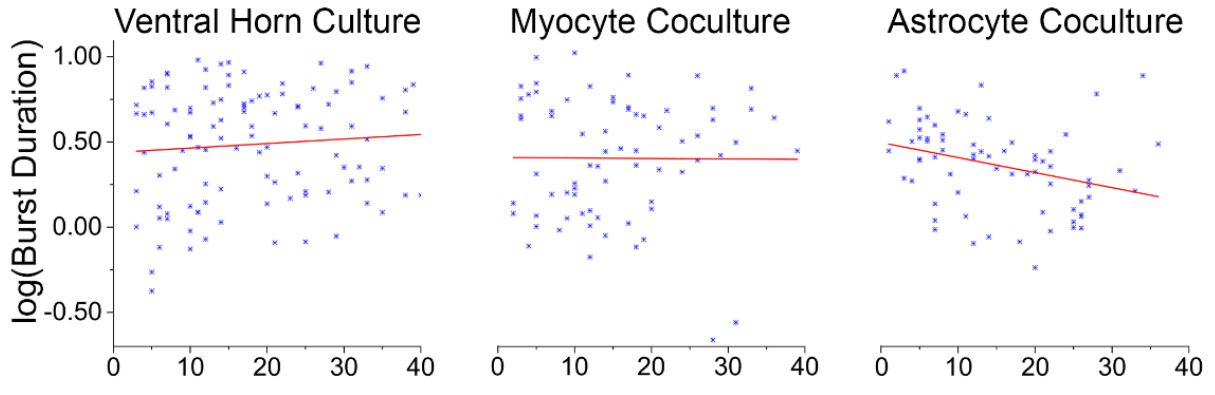


**Figure 22.** Average duration of bursts. Each point represents the average duration of all bursts recorded from all electrodes plotted versus time in vitro. Using Two-Way ANOVA, significant differences at $p<0.05$ were found between culture conditions. Burst Properties. Ventral horn cultures: 10 cultures, 107 recordings; Myocyte cocultures: 9 cultures, 72 recordings; Astrocyte cocultures: 7 cultures, 70 recordings.

cocultures to encode more complex messages, most likely through astrocyte regulation of

extracellular Ca2+ levels, suggests a progressive level of functional maturation (Morquette et al., 2015; Aoi Odawara, Gotoh, & Suzuki, 2013). The structural basis of this be due to an increase in synaptic connections. The recurrent connections would drive the connections.

The average duration of bursts was found to be significantly different ($p<0.05$) amongst culture types. Ventral horn cultures showed a lengthening of burst duration over days in vitro, while astrocytes showed even more significant shortening of burst duration (Fig. 22). Myocyte cocultures show little change with only a slight narrowing of duration over time. However, the true story doesn't play out unless interspike intervals are taken into consideration.

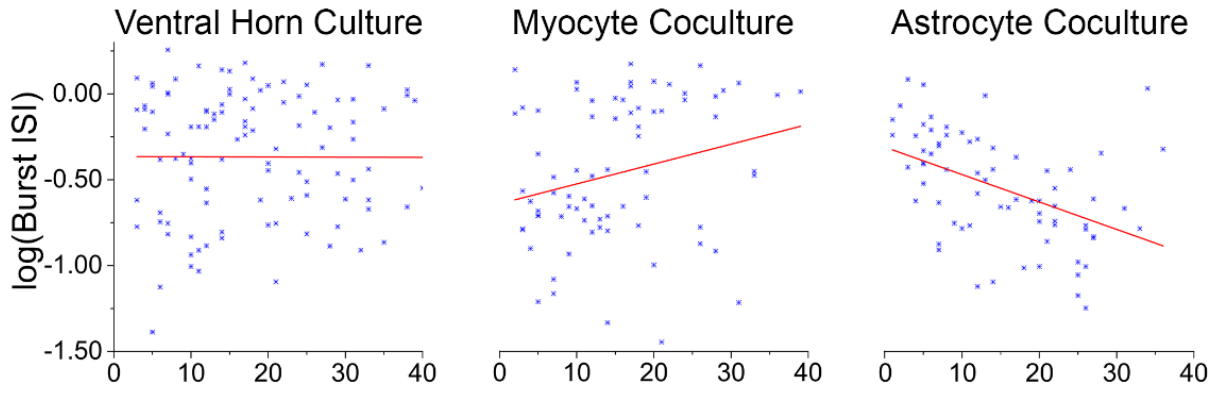


**Figure 23.** Mean interspike interval during bursts. Each point represents an average of the average ISI of each burst on all channels in the recording plotted versus time in vitro. Using Two-Way ANOVA significant differences at $p<0.05$ were found between culture conditions. Burst Properties. Ventral horn cultures: 10 cultures, 107 recordings; Myocyte cocultures: 9 cultures, 72 recordings; Astrocyte cocultures: 7 cultures, 70 recordings.

The time interval between spikes is called the interspike interval (ISI). For this metric we examined ISI between spikes recorded within a burst and then take the mean for each burst. ISI amongst conditions showed significant differences ($p<0.05$) between cultures (Fig. 23). Bonferonni post-hoc analysis showed significant ($p<0.05$) difference between ventral horn cultures and astrocyte cocultures. Ventral horn cultures showed almost no change in burst interspike interval over time (Fig. 23), while the average interspike interval for myocytes

cocultures increased over time, meaning that the spikes within a burst were more spread out in older cultures. Strikingly, for astrocyte cocultures, the interspike interval decreased over time, the opposite of myocyte cultures. Over time in culture, astrocyte cocultures moved toward a higher frequency train during bursts while myocyte cocultures moved toward a lower frequency train during burst. So, while both ventral horn cultures and myocyte cocultures show little change in burst duration, myocytes show a decreased concentration of spikes within bursts. Although no significant differences were found amongst the average number of spikes per burst, astrocyte cocultures have the fastest rate of increase followed by control and then myocyte cocultures (Fig. 24). This may signal a second stage of development after the neuron has formed a NMJ. After a NMJ is formed in vivo, increased spontaneous firing would result in pathologies such as fibrillations and fasciculations. Myocyte cocultures in vitro may pursue a similar progression. Over time, astrocyte cocultures show an increase in the number of bursts, a decrease in burst duration, and an increase in the frequency of spikes during the bursts, suggesting an

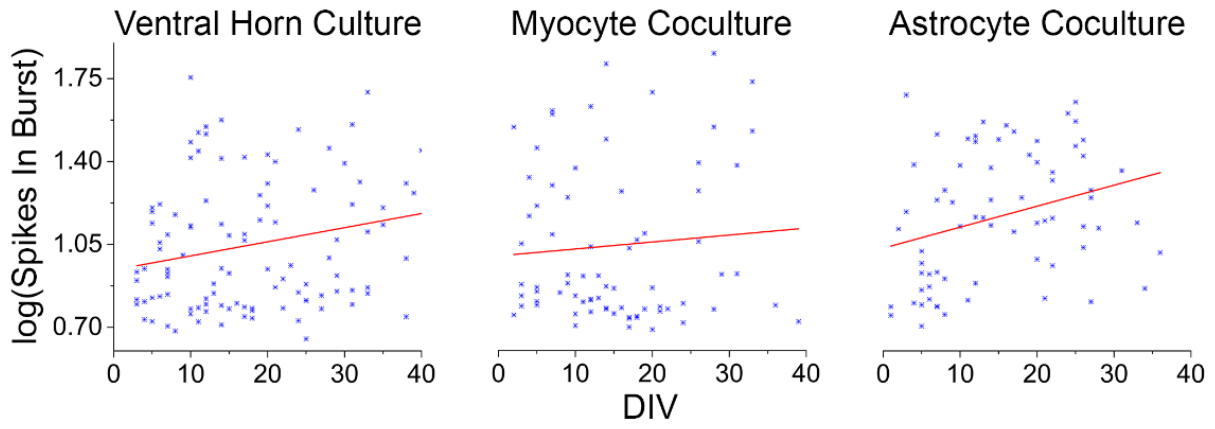


**Figure 24.** Average number of spikes per burst. Each point represents the average number of spikes per burst over all channels in the recording. Although no significant differences were seen, a visible trend can be seen with astrocyte cocultures showing the greatest rate of increase while myocyte cocultures show the least rate of increase. Ventral horn cultures: 10 cultures, 107 recordings; Myocyte cocultures: 9 cultures, 72 recordings; Astrocyte cocultures: 7 cultures, 70 recordings.

increase in intracellular network connectivity over time that may not occur in ventral horn and myocyte cocultures.

*5.4. Network Burst Characteristics*

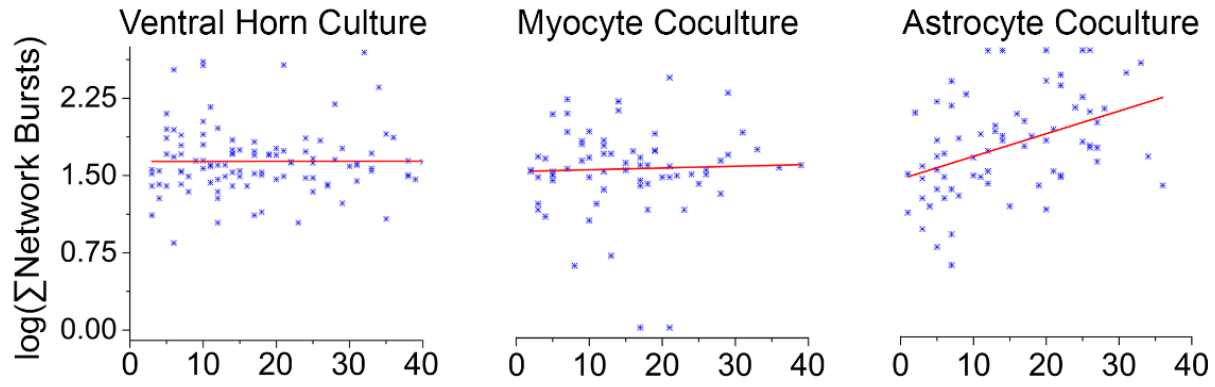


**Figure 25.** Sum number of network bursts. Each point represents the total number of network bursts across all channels in the recording on that day. Network bursting properties. Ventral horn cultures: 10 cultures, 107 recordings; Myocyte cocultures: 9 cultures, 72 recordings; Astrocyte cocultures: 7 cultures, 70 recordings.

Network bursts here are defined as the temporal overlap of six or more bursts from different sorted units. Network bursts can also be described as network synchronization, which is a correlation to recurrent synaptic connectivity and may be a more accurate representation of the creation of network activity patterns (Knudstrup, Zochowski, & Booth, 2016). Two-way ANOVA did not show significant differences ($p>0.05$) amongst cultures for the total number of network bursts, log(∑Network Bursts) in Fig. 25, but Bonferroni post-hoc analysis did discover significant differences ($p<0.05$) between myocyte cocultures and astrocyte cocultures. While muscle cocultures and astrocyte cocultures start at approximately the same level in the number of network bursts, astrocytes cocultures show an increase in the total number of network bursts over DIV compared to myocytes. The total number of network bursts per recording of ventral horn cultures showed relatively little change over time.

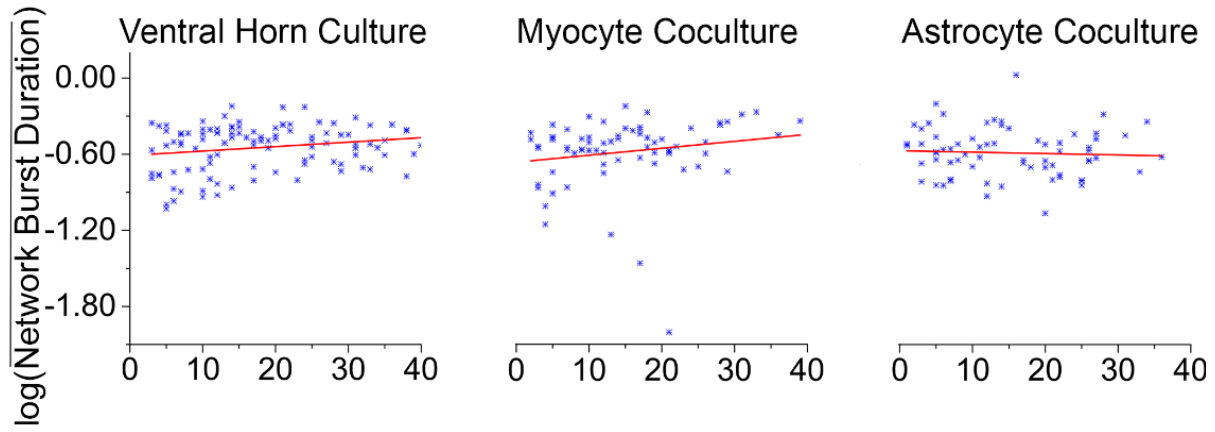


**Figure 26.** Average duration of network bursts. Each point represents the average duration of network bursts across all channels plotted versus days in vitro. Using Two-Way ANOVA at $p<0.05$ significant differences were found between DIV, but not between cultures. Network bursting properties. Ventral horn cultures: 10 cultures, 107 recordings; Myocyte cocultures: 9 cultures, 72 recordings; Astrocyte cocultures: 7 cultures, 70 recordings.

The mean duration of network bursts showed no significant ($p>0.05$) differences, either with two-way ANOVA or Bonferroni post-hoc analysis, between culture preparations. Two-way ANOVA analysis does point to significant ($p<0.05$) differences between DIV. Younger cultures appear to have an increased variance and a lower range of network burst durations than older cultures (Fig. 26). Although two-way ANOVA and post hoc analysis showed no significant

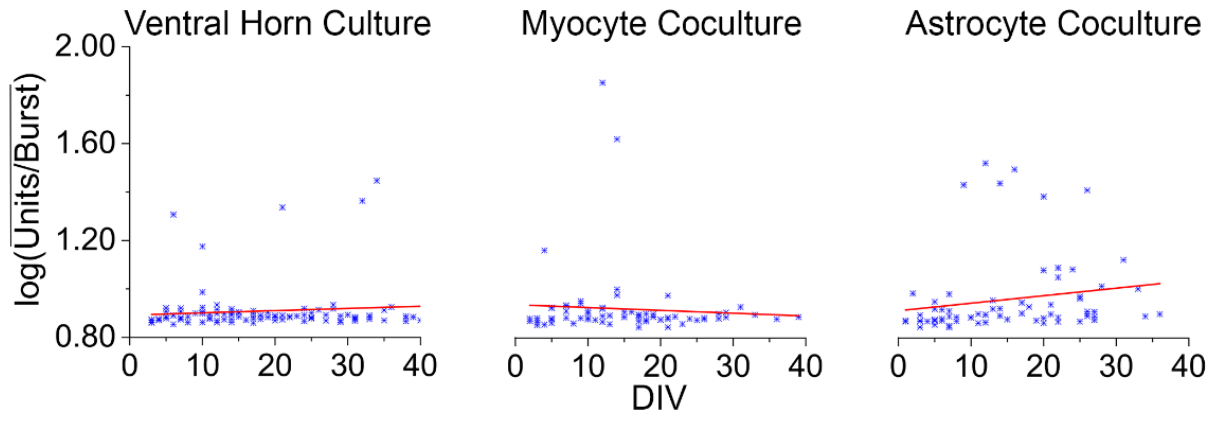


**Figure 27.** Average number of units involved in networks bursts. Each point represents the average number of channels involved in a network burst per recording plotted versus days in vitro. Network bursting properties. Ventral horn cultures: 10 cultures, 107 recordings; Myocyte cocultures: 9 cultures, 72 recordings; Astrocyte cocultures: 7 cultures, 70 recordings.

($p>0.05$) differences between cultures, it is interesting to note that the trend of myocyte cocultures follows ventral horn cultures of increasing in duration, while the trend of astrocytes moves in the opposite direction toward decreasing duration. Although no significant differences were seen in the average number of active units per network burst (Fig. 27), there does appear to be an upward trend over time in the number of channels with units participating in network bursts in astrocyte cocultures and a downward trend in the number of active channels in bursts in the muscle cocultures.

## CHAPTER VI: DISCUSSION

Neuronal cell culture has been an important tool in the biological sciences for almost three quarters of a century, and has been critical in expanding our understanding of the physiology and cell biology of neurons (Weiss, 1945). Culture systems make excellent models because a single cell type can be isolated and multiple variables influencing cell's development or death can be controlled by an investigator. Such closed systems are helpful when examining very specific cellular or molecular mechanisms. However, that same closed system may be an impediment when evaluating how neurons behave as part of a network activity. For example, in the case of motor neurons, production and release of acetylcholine is currently the gold standard by which we identify motor neurons, however motor neurons in culture release primarily glutamate (H. Zhang, Wu, Wang, & Harrington, 2011). In addition, acetylcholine plays an important role in development to construct spinal locomotor circuits and regulate axonal growth and pre-synaptic specialization (An et al., 2010; Myers et al., 2005) while acetylcholine esterase (AChE) is important for the production of acetylcholine. It has been shown that NMJ formation of rat spinal neurons with human muscles, the largest fraction of AChE contribution coming from the muscle (Jevsek et al., 2004). In culture, with minimal influence of AChE from muscle, motor neurons are likely missing important developmental signals. It has also been shown that human induced pluripotent stem cell (hiPSC) derived motor neurons, motor neuron like cell-lines, and dorsal root ganglion sensory neurons can all form neuromuscular junctions when cocultured with myocytes (Demestre et al., 2015; Liu et al., 2011; O'Connor et al., 2018). If production of acetylcholine is a major characteristic by which motor neuron networks are classified and if most of the AChE contribution comes from the muscle, then a motor neuron network model *in vitro* without the presence of muscle, is not an accurate model of a motor neuron network *in vivo*. We

show that the impact of the presence of muscle is apparent in the functional output of a developing motor neuron network.

With the increasing amount of literature suggesting that astrocytes play an integral part of a neural network, the same logic can be applied to *in vitro* neural network models lacking astrocytes. Neural models using cell lines or hIPSC that do not include a critical mass of astrocytes might not represent an accurate model of the development and function of an in vivo network. We show dramatic functional changes in developing neural network activity when astrocyte levels are increased by coculture. It maybe that the presence of myocytes or astrocytes push a developing motor neuron network to maturation (Brandebura et al., 2018; Farhy-Tselnicker & Allen, 2018; Tomàs et al., 2017), while the endpoints appear to be functionally distinct between muscle cocultures and astrocyte cocultures.

Although there will naturally be variability in our data, as expected in any biological system, our large sample size and a focus on trends minimizes this limitation. Plating a high concentration of ventral horn neurons improves networking, but the number of plated neurons does not always correlate with the number anchored, networked neurons weeks later. However, consistency in plating protocol provides internal validity. Automated spike sorting is a constantly changing field with no real gold standard at the moment. Using widely accepted methods in an undeviating fashion provides a measure of internal validity unachievable by manual sorting.

Initially all culture conditions start at approximately the same level of active units, approximately 1.96 to 1.99 log(∑Total Units). Because each unit is assumed to represent a unique neuron, one can consider that the number of active nodes of each network are approximately equal across all culture conditions soon after plating. However over time, ventral horn cultures show a slight increase in the number of units recorded over 40 days (Fig. 16).

Myocyte cocultures showed an almost 57% increase in slope of line of fit as compared with ventral horn cultures. Astrocyte cocultures showed a slight decrease in units over time. A previous study showed similar results, in that they found a decrease in number of detected electrodes over a 35 days period with astrocyte cocultures (A. Odawara, Saitoh, Alhebshi, Gotoh, & Suzuki, 2014). It's also been shown that primary neural cultures that are not cocultured with astrocytes will also initially show diffuse spontaneous activity, but over time the network will consolidate to fewer active neurons (Soriano, Rodriguez Martinez, Tlusty, & Moses, 2008). It has been shown that astrocytes are required for neuronal maturation and synapse formation (Lischka et al., 2018; Pyka, Busse, Seidenbecher, Gundelfinger, & Faissner, 2011; Xia, Zhu, Shevelkin, Ross, & Pletnikov, 2016). The similarities we see between the astrocyte cocultures and ventral horn cultures may be because they are both moving toward the same functional end point, but that process is accelerated by astrocytes.

The ventral horn cultures are very similar to the astrocyte cultures in cell type composition but vary greatly in concentration of astrocytes. The increased concentration of astrocytes in cocultures may be leading to an increased rate of circuit development that may more closely mimic in vivo situations in ratio of astrocytes to neurons (Herculano-Houzel, 2005). It is interesting to note that ventral horn cultures trend in the opposite direction of astrocyte cocultures regarding total units, average duration of bursts, and average duration of network bursts. It has been suggested that a decrease in burst duration may actually increase the informational coding capacity of a network (Tinkhauser et al., 2017). The reduction in units may be a function of energy constraints seen both *in vivo* as well as *in vitro*. Neural tissue consumes energy at a higher rate than cardiac tissue (Ames, 2000). In adult humans approximately 20% of resting energy consumption is utilized by the brain, while in infants it's closer to 60%;

suggesting metabolic demands may be a limiting factor in brain size (Hofman, 1983). If system economy can be improved by reducing the number of neural units in a network, then elimination of redundancy will reduce the biological currency required by the system while not suffering from informational packet loss (Laughlin & Sejnowski, 2003).

We've found that over time astrocyte cocultured networks act quite differently than older myocyte cocultured networks, while ventral horn cultures usually fall in between the two cocultures on most metrics. This may be because the functional endpoint in a motor neuron networks is quite distinct from other neural cell types. Myocyte cocultures have a slightly more rapidly increasing number of sorted units compared to ventral horn cocultures. This is stark contrast to many other spiking metrics of muscle co-cultures which show a decrease over time such as total spikes, average amplitude, average energy, and total energy of recording. After a neuron forms a neuromuscular junction, there is in an increase in acetylcholinesterase, which then leads to an increase in acetylcholine, which then negatively regulates synapse formation (An et al., 2010; Lin et al., 2005). This is a sign of motor neuron network differentiation. The synaptic inhibition of acetylcholine is also the most likely cause of muscle cocultures showing the only decrease over time in channels involved in a network burst. The increase in unit number seen in plain ventral horn cultures and myocyte cocultures may be due to motor neuron progenitors maturing into functional motor neurons, however the decrease in units seen amongst astrocyte cocultures maybe due to a subpopulation of cells with pluripotent status differentiating into generic glutamatergic neurons (H. Zhang et al., 2011). So, while there is an increase in number of active neurons, there is a decrease in overall firing and in neurons involved in network bursts. This appears to be the key signature of a differentiated motor neuron network in vitro.

Although all efforts were taken to isolate the ventral portion of the spinal cord, we can say with a fair bit of certainty that other neural cell types were most likely also isolated. Even if other neural cell types, besides motor neurons, were inadvertently collected these neurons may still form a neuromuscular junction. It has been found that NMJs will also form when the sensory terminals of a spinal dorsal root ganglion are cocultured with muscle (Liu et al., 2011). In the presence of muscle the drive to create a NMJ is strong and will occur in human induced pluripotent stem cells (hIPSCs) derived motor neurons (Demestre et al., 2015), cholinergic cell lines (Jiang et al., 2003), across species (Jevsek et al., 2004), and through microfluidic channels (Zahavi et al., 2015). The presence of muscular components will also push neurons capable of producing acetylcholine to increase expression of acetylcholinesterase (Jiang et al., 2003), whose origin is of both muscle fiber and neuronal (Jevsek et al., 2004). It appears no matter the initial neural cell type, a collection of neurons exposed to muscle in vitro will differentiate into a motor neuron network. Our results suggest that the presence of NMJs appears to have a compounding inhibitory effect on network activity over a 40-day duration. Although presently of unknown etiology, possible origins could be due to activity-dependent elimination of neuromuscular junctions, which in other work has be shown to cause a 7.6% loss in unstimulated preparations over a period of 3 days (Nelson, Fields, Yu, & Liu, 1993). A developing network may benefit from having a more distributed number of weaker nodes, rather than a select few that are stronger.

The total number of spikes showed little change over time in ventral horn cultures, while myocyte cocultures and astrocyte cocultures showed opposing changes in total spike counts over time (Fig. 17). While astrocyte cocultures showed an increase in total spikes, myocytes cocultures showed a decline. The increase in activity of spikes seen over time when neurons

were cultured with astrocytes may again be possibly attributed to network maturation and is also seen in other studies (A. Odawara et al., 2014). All cultures contain astrocytes, however the astrocyte cocultures have a much larger proportion than the ventral horn cultures. The dramatic negative trend seen on most metrics for myocyte cocultures must be due to the presence of neuromuscular junctions, since the presence of muscle is the only significant difference between culture preparations. As neurons become more motor neuron like the level of spontaneous firing should fall to the low levels seen *in vivo*. Ventral horn, as well as astrocytes cocultures, showed almost no change over time for number of spikes detected (Fig. 17), but did show an increase of amplitude in those detected spikes (Fig. 18). The increase in amplitude of extracellular potential does suggest that some change is occurring over time, and that it may be due to an increase in size of the neurons in culture, a change in the proportion of larger versus smaller neurons, or the number of active neurons close to the electrodes. Although the amplitude of intracellular voltage change of any neural cell type during an action potential should be constant, there can be variation in the size of those neurons. That differences in cell size will be reflected in a corresponding change in amplitude of the extracellular potentials. In addition, if there is an increase in the active neural cell count over time, that will also correspond to an increase in amplitude of detected spikes due to overlapping spikes, which will have an additive effect on the peak to valley distance of the spike. Based on these assumptions, the decrease in amplitude seen amongst myocyte cocultures (Fig. 18) is most likely due to a decrease in the number of active neurons and/or a decrease in size of those neurons.

Changes in spike frequency and spike amplitude are reflected in the changes seen with average spike energy (Fig. 19) and total energy (Fig. 20) emitted by the cultures over the five-minute recording. Although the change in energy per waveform and the total sum energy of all

waveforms follow the same trend, the sum energy of a full recording shows a more rapid increase in astrocyte cocultures and a more rapid decrease in myocyte cocultures. The increase in the absolute value of mean energy of detected spikes versus sum energy amongst astrocyte and myocyte cocultures is due to similar changes in spiking frequency seen in those culture types. While the mean energy of a waveform takes the mean amplitude of spikes as a factor, the sum energy of a recording takes both the mean amplitude of spikes and mean energy as a factor. Since the spike frequency of control ventral horn cultures (Fig. 17) shows little change over time, there is little change seen amongst the slopes of mean amplitude of spikes (Fig. 18), mean energy of spikes (Fig. 19), or the sum energy of spikes (Fig. 20) amongst ventral horn control cultures.

Overall, we see dramatic changes in ventral horn neurons when cultured with astrocytes or myocytes. On most measures of neuronal and network activity, myocyte cocultures will decrease over time while astrocyte cocultures will increase over time. While it is true that neuromuscular junctions were not specifically stained for, the mere presence of muscle with any neural cell type is a strong force for formation of neuromuscular junctions (Demestre et al., 2015; Jevsek et al., 2004; Liu et al., 2011; Zahavi et al., 2015). That in turn drives those neurons to produce acetylcholinesterase and subsequently acetylcholine (Jevsek et al., 2004; Jiang et al., 2003). The increase in acetylcholine then negatively regulates axon growth, presynaptic specialization, and synapse formation which may be the cause for network inhibition seen amongst myocyte cocultures (An et al., 2010; Lin et al., 2005). While astrocyte cocultures may have increase network activity due to induction of synapse formation, synapse maturation, attenuation of releasable pool of synaptic vesicles, increase in autaptic glutamate release, and an increase in astrocytic $Ca^{2+}$ (Kawano et al., 2012; A. Odawara et al., 2014; Szabó et al., 2017). The measurable functional changes seen in ventral horn neurons when cocultured with myocytes

suggest that an in vitro motor neuron model requires the presence of muscle to more closely replicate an in vivo motor neuron network. The same sentiment applies to astrocytes and all neuronal cultures. In mammalian biology, neurons always work in conjunction with astrocytes. Without the presence of astrocytes, such as in cell lines or induced pluripotent stem cells, an in vitro neural network is not a functionally accurate model of an in vivo neuronal network. Based on the data, the most accurate *in vitro* lower motor neuron model would most likely be a combination of what was done here; a coculture of spinal motor neurons with both myocytes as well as significantly increased levels of astrocytes.

## REFERENCES


Aebersold, M. J., Thompson-Steckel, G., Joutang, A., Schneider, M., Burchert, C., Forró, C., … Vörös, J. (2018). Simple and Inexpensive Paper-Based Astrocyte Co-culture to Improve Survival of Low-Density Neuronal Networks. *Frontiers in Neuroscience*, *12*(February), 1–14. https://doi.org/10.3389/fnins.2018.00094

Akemann, W. (2006). Interaction of Kv3 Potassium Channels and Resurgent Sodium Current Influences the Rate of Spontaneous Firing of Purkinje Neurons. *Journal of Neuroscience*, *26*(17), 4602–4612. https://doi.org/10.1523/JNEUROSCI.5204-05.2006

Ames, A. (2000). CNS energy metabolism as related to function. *Brain Research. Brain Research Reviews*, *34*(1–2), 42–68. Retrieved from http://www.sciencedirect.com/science/article/pii/S0165017300000382

Amin, H., Maccione, A., Marinaro, F., Zordan, S., Nieus, T., & Berdondini, L. (2016). Electrical Responses and Spontaneous Activity of Human iPS-Derived Neuronal Networks Characterized for 3-month Culture with 4096-Electrode Arrays. *Frontiers in Neuroscience*, *10*(MAR). https://doi.org/10.3389/fnins.2016.00121

An, M. C., Lin, W., Yang, J., Dominguez, B., Padgett, D., Sugiura, Y., … Lee, K.-F. (2010). Acetylcholine negatively regulates development of the neuromuscular junction through distinct cellular mechanisms. *Proceedings of the National Academy of Sciences*, *107*(23), 10702–10707. https://doi.org/10.1073/pnas.1004956107

Bahmani, L., Taha, M. F., & Javeri, A. (2014). Coculture with embryonic stem cells improves neural differentiation of adipose tissue-derived stem cells. *Neuroscience*, *272*, 229–239. https://doi.org/10.1016/j.neuroscience.2014.04.063

Bogdanowicz, D. R., & Lu, H. H. (2013). Studying cell-cell communication in co-culture. *Biotechnology Journal*, *8*(4), 395–396. https://doi.org/10.1002/biot.201300054

Brandebura, A. N., Morehead, M., Holcomb, P., Heller, D. T., Kolson, D. R., Jones, G., … Spirou, G. A. (2018). Glial cell expansion coincides with neural circuit formation in the developing auditory brainstem. *Developmental Neurobiology*, 0–1. https://doi.org/10.1002/dneu.22633

Buzsáki, G. (2004). Large-scale recording of neuronal ensembles. *Nature Neuroscience*, *7*(5), 446–451. https://doi.org/10.1038/nn1233

Campenot, R. B. (1977). Local control of neurite development by nerve growth factor. *Proceedings of the National Academy of Sciences of the United States of America*, *74*(10), 4516–4519. https://doi.org/10.1073/pnas.74.10.4516

Carlson, D., & Carin, L. (2019). Continuing progress of spike sorting in the era of big data. *Current Opinion in Neurobiology*, *55*, 90–96. https://doi.org/10.1016/j.conb.2019.02.007

Cashman, N. R., Durham, H. D., Blusztajn, J. K., Oda, K., Tabira, T., Shaw, I. T., … Antel, J. P. (1992). Neuroblastoma x spinal cord (NSC) hybrid cell lines resemble developing motor neurons. *Developmental Dynamics : An Official Publication of the American Association of Anatomists*, *194*(3), 209–221. https://doi.org/10.1002/aja.1001940306

Chelaru, M. I., & Jog, M. S. (2005). Spike source localization with tetrodes. *Journal of Neuroscience Methods*, *142*(2), 305–315. https://doi.org/10.1016/j.jneumeth.2004.09.004

Chen, S., Hong, X., & Harris, C. J. (2004). Sparse kernel density construction using orthogonal forward regression with leave-one-out test score and local regularization. *IEEE*

*Transactions on Systems, Man, and Cybernetics. Part B, Cybernetics : A Publication of the IEEE Systems, Man, and Cybernetics Society*, *34*(4), 1708–1717. Retrieved from http://www.ncbi.nlm.nih.gov/pubmed/15462438

Davis-Dusenbery, B. N., Williams, L. A., Klim, J. R., & Eggan, K. (2014). How to make spinal motor neurons. *Development (Cambridge, England)*, *141*(3), 491–501. https://doi.org/10.1242/dev.097410

Demestre, M., Orth, M., Föhr, K. J., Achberger, K., Ludolph, A. C., Liebau, S., & Boeckers, T. M. (2015). Formation and characterisation of neuromuscular junctions between hiPSC derived motoneurons and myotubes. *Stem Cell Research*, *15*(2), 328–336. https://doi.org/10.1016/j.scr.2015.07.005

Dempster, A. P., Laird, N. M., & Rubin, D. B. (1977). Maximum Likelihood from Incomplete Data Via the EM Algorithm . In *Journal of the Royal Statistical Society: Series B (Methodological)* (Vol. 39). https://doi.org/10.1111/j.2517-6161.1977.tb01600.x

Duin. (1976). On the Choice of Smoothing Parameters for Parzen Estimators of Probability Density Functions. *IEEE Transactions on Computers*, *C–25*(11), 1175–1179. https://doi.org/10.1109/TC.1976.1674577

Einevoll, G. T., Franke, F., Hagen, E., Pouzat, C., & Harris, K. D. (2012). Towards reliable spike-train recordings from thousands of neurons with multielectrodes. *Current Opinion in Neurobiology*, *22*(1), 11–17. https://doi.org/10.1016/j.conb.2011.10.001

Engel, K., & Hanisch, S. (2014). Reconstruction of cell-electrode-adjacencies on multielectrode arrays. *Journal of Computational Neuroscience*, *37*(3), 583–591. https://doi.org/10.1007/s10827-014-0524-6

Farhy-Tselnicker, I., & Allen, N. J. (2018). Astrocytes, neurons, synapses: a tripartite view on cortical circuit development. *Neural Development*, *13*(1), 7. https://doi.org/10.1186/s13064-018-0104-y

Fogarty, M. J., Mu, E. W. H., Noakes, P. G., Lavidis, N. A., & Bellingham, M. C. (2016). Marked changes in dendritic structure and spine density precede significant neuronal death in vulnerable cortical pyramidal neuron populations in the SOD1G93A mouse model of amyotrophic lateral sclerosis. *Acta Neuropathologica Communications*, *4*(1), 1–21. https://doi.org/10.1186/s40478-016-0347-y

Forgy, E. W. (1965). Cluster Analysis of Multivariate Data: Efficiency vs. Interpretability of Classifications. *Biometrics*, *21*(3), 768–769. Retrieved from http://www.jstor.org/stable/2528559

Franke, F., Natora, M., Boucsein, C., Munk, M. H. J., & Obermayer, K. (2010). An online spike detection and spike classification algorithm capable of instantaneous resolution of overlapping spikes. *Journal of Computational Neuroscience*, *29*(1–2), 127–148. https://doi.org/10.1007/s10827-009-0163-5

Gagnon-Turcotte, G., & Gosselin, B. (2015). Multichannel spike detector with an adaptive threshold based on a Sigma-delta control loop. *2015 37th Annual International Conference of the IEEE Engineering in Medicine and Biology Society (EMBC)*, *2015*(418), 7123–7126. https://doi.org/10.1109/EMBC.2015.7320034

Gerstein, G. L., & Clark, W. A. (1964). Simultaneous Studies of Firing Patterns in Several Neurons. *Science*, *143*(3612), 1325–1327. https://doi.org/10.1126/science.143.3612.1325

Gray, C. M., Maldonado, P. E., Wilson, M., & McNaughton, B. (1995). Tetrodes markedly

improve the reliability and yield of multiple single-unit isolation from multi-unit recordings in cat striate cortex. *Journal of Neuroscience Methods*, *63*(1–2), 43–54. https://doi.org/10.1016/0165-0270(95)00085-2

Grieco, T. M. (2004). Production of Resurgent Current in NaV1.6-Null Purkinje Neurons by Slowing Sodium Channel Inactivation with -Pompilidotoxin. *Journal of Neuroscience*, *24*(1), 35–42. https://doi.org/10.1523/JNEUROSCI.3807-03.2004

Gullo, F., Maffezzoli, A., Dossi, E., & Wanke, E. (2009). Short-latency cross- and autocorrelation identify clusters of interacting cortical neurons recorded from multi-electrode array. *Journal of Neuroscience Methods*, *181*(2), 186–198. https://doi.org/10.1016/j.jneumeth.2009.05.003

Haghiri, S., Ahmadi, A., & Saif, M. (2017). Complete Neuron-Astrocyte Interaction Model: Digital Multiplierless Design and Networking Mechanism. *IEEE Transactions on Biomedical Circuits and Systems*, *11*(1), 117–127. https://doi.org/10.1109/TBCAS.2016.2583920

Herculano-Houzel, S. (2005). Isotropic Fractionator: A Simple, Rapid Method for the Quantification of Total Cell and Neuron Numbers in the Brain. *Journal of Neuroscience*, *25*(10), 2518–2521. https://doi.org/10.1523/JNEUROSCI.4526-04.2005

Hofman, M. A. (1983). Energy metabolism, brain size and longevity in mammals. *The Quarterly Review of Biology*, *58*(4), 495–512. Retrieved from http://www.ncbi.nlm.nih.gov/pubmed/6665118

Hong, X., Chen, S., & Harris, C. J. (2008). A forward-constrained regression algorithm for sparse kernel density estimation. *IEEE Transactions on Neural Networks*, *19*(1), 193–198.

https://doi.org/10.1109/TNN.2007.908645

Hovey, M. M., Bak, A. F., & Carpenter, D. O. (1972). Low internal conductivity of Aplysia neuron somata. *Science (New York, N.Y.)*, *176*(4041), 1329–1331. https://doi.org/10.1126/science.176.4041.1329

Hu, B. Y., & Zhang, S. C. (2009). Differentiation of spinal motor neurons from pluripotent human stem cells. *Nature Protocols*, *4*(9), 1295–1304. https://doi.org/10.1038/nprot.2009.127

Hyung, S., Yoon Lee, B., Park, J.-C., Kim, J., Hur, E.-M., & Francis Suh, J.-K. (2015). Coculture of Primary Motor Neurons and Schwann Cells as a Model for In Vitro Myelination. *Scientific Reports*, *5*, 15122. https://doi.org/10.1038/srep15122

Iadecola, C. (2017). The Neurovascular Unit Coming of Age: A Journey through Neurovascular Coupling in Health and Disease. *Neuron*, *96*(1), 17–42. https://doi.org/10.1016/j.neuron.2017.07.030

Im, G.-I. (2014). Coculture in Musculoskeletal Tissue Regeneration. *Tissue Engineering Part B: Reviews*, *20*(5), 545–554. https://doi.org/10.1089/ten.teb.2013.0731

Ionescu, A., Zahavi, E. E., Gradus, T., Ben-Yaakov, K., & Perlson, E. (2016). Compartmental microfluidic system for studying muscle–neuron communication and neuromuscular junction maintenance. *European Journal of Cell Biology*, *95*(2), 69–88. https://doi.org/10.1016/j.ejcb.2015.11.004

Jevsek, M., Mars, T., Mis, K., & Grubic, Z. (2004). Origin of acetylcholinesterase in the neuromuscular junction formed in the in vitro innervated human muscle. *European Journal*

*of Neuroscience*, *20*(11), 2865–2871. https://doi.org/10.1111/j.1460-9568.2004.03752.x

Jiang, J. X. S., Choi, R. C. Y., Siow, N. L., Lee, H. H. C., Wan, D. C. C., & Tsim, K. W. K. (2003). Muscle induces neuronal expression of acetylcholinesterase in neuron-muscle co-culture: Transcriptional regulation mediated by camp-dependent signaling. *Journal of Biological Chemistry*, *278*(46), 45435–45444. https://doi.org/10.1074/jbc.M306320200

Johnson, M. A., Weick, J. P., Pearce, R. A., & Zhang, S.-C. (2007). Functional neural development from human embryonic stem cells: accelerated synaptic activity via astrocyte coculture. *The Journal of Neuroscience : The Official Journal of the Society for Neuroscience*, *27*(12), 3069–3077. https://doi.org/10.1523/JNEUROSCI.4562-06.2007

Kawano, H., Katsurabayashi, S., Kakazu, Y., Yamashita, Y., Kubo, N., Kubo, M., … Iwasaki, K. (2012). Long-Term Culture of Astrocytes Attenuates the Readily Releasable Pool of Synaptic Vesicles. *PLoS ONE*, *7*(10). https://doi.org/10.1371/journal.pone.0048034

Kerschensteiner, D. (2014). Spontaneous Network Activity and Synaptic Development. *The Neuroscientist : A Review Journal Bringing Neurobiology, Neurology and Psychiatry*, *20*(3), 272–290. https://doi.org/10.1177/1073858413510044

Kim, K. H., & Kim, S. J. (2000). Neural spike sorting under nearly 0-dB signal-to-noise ratio using nonlinear energy operator and artificial neural-network classifier. *IEEE Transactions on Bio-Medical Engineering*, *47*(10), 1406–1411. https://doi.org/10.1109/10.871415

Kim, M. D., Wen, Y., & Jan, Y. N. (2009). Patterning and organization of motor neuron dendrites in the Drosophila larva. *Developmental Biology*, *336*(2), 213–221. https://doi.org/10.1016/j.ydbio.2009.09.041

Kim, S. U., Oh, T. H., & Johnson, D. D. (1972). Developmental changes of acetylcholinesterase and pseudocholinesterase in organotypic cultures of spinal cord. *Experimental Neurology*, *35*(2), 274–281. https://doi.org/10.1016/0014-4886(72)90153-7

Kloosterman, F., Layton, S. P., Chen, Z., & Wilson, M. A. (2013). Bayesian decoding using unsorted spikes in the rat hippocampus. *Journal of Neurophysiology*, *111*(1), 217–227. https://doi.org/10.1152/jn.01046.2012

Knudstrup, S., Zochowski, M., & Booth, V. (2016). Network burst dynamics under heterogeneous cholinergic modulation of neural firing properties and heterogeneous synaptic connectivity. *European Journal of Neuroscience*, *43*(10), 1321–1339. https://doi.org/10.1111/ejn.13210

Koontz, W. L. G., & Fukunaga, K. (1972). A Nonparametric Valley-Seeking Technique for Cluster Analysis. *IEEE Transactions on Computers*, *C–21*(2), 171–178. https://doi.org/10.1109/TC.1972.5008922

Kreiter, A. K., Aertsen, A. M. H. J., & Gerstein, G. L. (1989). A low-cost single-board solution for real-time, unsupervised waveform classification of multineuron recordings. *Journal of Neuroscience Methods*, *30*(1), 59–69. https://doi.org/10.1016/0165-0270(89)90075-7

Krencik, R., Seo, K., van Asperen, J. V., Basu, N., Cvetkovic, C., Barlas, S., … Ullian, E. M. (2017). Systematic Three-Dimensional Coculture Rapidly Recapitulates Interactions between Human Neurons and Astrocytes. *Stem Cell Reports*, *9*(6), 1745–1753. https://doi.org/10.1016/j.stemcr.2017.10.026

Laughlin, S. B., & Sejnowski, T. J. (2003). Communication in neuronal networks. *Science (New York, N.Y.)*, *301*(5641), 1870–1874. https://doi.org/10.1126/science.1089662

Legendy, C. R., & Salcman, M. (1985). Bursts and recurrences of bursts in the spike trains of spontaneously active striate cortex neurons. *Journal of Neurophysiology*, *53*(4), 926–939. https://doi.org/10.1152/jn.1985.53.4.926

Lewicki, M. S. (1998). A review of methods for spike sorting: the detection and classification of neural action potentials. *Network (Bristol, England)*, *9*(4), R53-78. Retrieved from http://www.ncbi.nlm.nih.gov/pubmed/10221571

Lin, W., Dominguez, B., Yang, J., Aryal, P., Brandon, E. P., Gage, F. H., & Lee, K. F. (2005). Neurotransmitter acetylcholine negatively regulates neuromuscular synapse formation by a Cdk5-dependent mechanism. *Neuron*, *46*(4), 569–579. https://doi.org/10.1016/j.neuron.2005.04.002

Lischka, F. W., Efthymiou, A., Zhou, Q., Nieves, M. D., McCormack, N. M., Wilkerson, M. D., … Doughty, M. L. (2018). Neonatal mouse cortical but not isogenic human astrocyte feeder layers enhance the functional maturation of induced pluripotent stem cell-derived neurons in culture. *Glia*, *66*(4), 725–748. https://doi.org/10.1002/glia.23278

Lisman, J. E. (1997). Bursts as a unit of neural information: Making unreliable synapses reliable. *Trends in Neurosciences*, *20*(1), 38–43. https://doi.org/10.1016/S0166-2236(96)10070-9

Liu, H., Wang, L., Li, H., Liu, Z., Wang, H., & Li, Z. (2011). Formation of Neuromuscular Junction-Like Structure Between Primary Sensory Terminals and Skeletal Muscle Cells in Vitro. *Anatomical Record*, *294*(3), 472–478. https://doi.org/10.1002/ar.21310

Lloyd, S. (1982). Least squares quantization in PCM. *IEEE Transactions on Information Theory*, *28*(2), 129–137. https://doi.org/10.1109/TIT.1982.1056489

Mankin, R. W., Grant, A. J., & Mayer, M. S. (1987). A microcomputer-controlled response measurement and analysis system for insect olfactory receptor neurons. *Journal of Neuroscience Methods*, *20*(4), 307–322. https://doi.org/10.1016/0165-0270(87)90063-X

Martinello, T., & Patruno, M. (2008). Embryonic chick cocultures of neuronal and muscle cells. *Neurological Research*, *30*(2), 179–182. https://doi.org/10.1179/174313208X281064

Matsumoto, a., Yoshino, H., Yuki, N., Hara, Y., Cashman, N. R., Handa, S., & Miyatake, T. (1995). Ganglioside characterization of a cell line displaying motor neuron-like phenotype: GM2 as a possible major ganglioside in motor neurons. *Journal of the Neurological Sciences*, *131*(2), 111–118. https://doi.org/10.1016/0022-510X(95)00267-X

Mavel, S., Vourc'h, P., Potier-Cartereau, M., Patin, F., Guéguinou, M., Felix, R., … Blasco, H. (2016). NSC-34 Motor Neuron-Like Cells Are Unsuitable as Experimental Model for Glutamate-Mediated Excitotoxicity. *Frontiers in Cellular Neuroscience*, *10*(May), 1–12. https://doi.org/10.3389/fncel.2016.00118

Mechler, F., Victor, J. D., Ohiorhenuan, I., Schmid, A. M., & Hu, Q. (2011). Three-dimensional localization of neurons in cortical tetrode recordings. *Journal of Neurophysiology*, *106*(2), 828–848. https://doi.org/10.1152/jn.00515.2010

Mechler, Ferenc, & Victor, J. D. (2012). Dipole characterization of single neurons from their extracellular action potentials. *Journal of Computational Neuroscience*, *32*(1), 73–100. https://doi.org/10.1007/s10827-011-0341-0

Miki, Y., Ono, K., Hata, S., Suzuki, T., Kumamoto, H., & Sasano, H. (2012). The advantages of co-culture over mono cell culture in simulating in vivo environment. *Journal of Steroid Biochemistry and Molecular Biology*, *131*(3–5), 68–75.

https://doi.org/10.1016/j.jsbmb.2011.12.004

Milekovic, T., Sarma, A. A., Bacher, D., Simeral, J. D., Saab, J., Pandarinath, C., … Hochberg, L. R. (2018). Stable long-term BCI-enabled communication in ALS and locked-in syndrome using LFP signals. *Journal of Neurophysiology*, *120*(1), 343–360. https://doi.org/10.1152/jn.00493.2017

Milligan, C., & Gifondorwa, D. (2011). Isolation and culture of postnatal spinal motoneurons. *Methods in Molecular Biology (Clifton, N.J.)*, *793*, 77–85. https://doi.org/10.1007/978-1-61779-328-8_5

Milner, L. D., & Landmesser, L. T. (1999). Cholinergic and GABAergic inputs drive patterned spontaneous motoneuron activity before target contact. *The Journal of Neuroscience : The Official Journal of the Society for Neuroscience*, *19*(8), 3007–3022. Retrieved from http://www.ncbi.nlm.nih.gov/pubmed/10191318

Morquette, P., Verdier, D., Kadala, A., Féthière, J., Philippe, A. G., Robitaille, R., & Kolta, A. (2015). An astrocyte-dependent mechanism for neuronal rhythmogenesis. *Nature Neuroscience*, *18*(6), 844–854. https://doi.org/10.1038/nn.4013

Myers, C. P., Lewcock, J. W., Hanson, M. G., Gosgnach, S., Aimone, J. B., Gage, F. H., … Pfaff, S. L. (2005). Cholinergic input is required during embryonic development to mediate proper assembly of spinal locomotor circuits. *Neuron*, *46*(1), 37–49. https://doi.org/10.1016/j.neuron.2005.02.022

Nelson, P. G., Fields, R. D., Yu, C., & Liu, Y. (1993). Synapse elimination from the mouse neuromuscular junction in vitro: A non-hebbian activity-dependent process. *Journal of Neurobiology*, *24*(11), 1517–1530. https://doi.org/10.1002/neu.480241106

O'Connor, E., Phan, V., Cordts, I., Cairns, G., Hettwer, S., Cox, D., … Roos, A. (2018). MYO9A deficiency in motor neurons is associated with reduced neuromuscular agrin secretion. *Human Molecular Genetics*, *27*(8), 1434–1446. https://doi.org/10.1093/hmg/ddy054

Odawara, A., Saitoh, Y., Alhebshi, A. H., Gotoh, M., & Suzuki, I. (2014). Long-term electrophysiological activity and pharmacological response of a human induced pluripotent stem cell-derived neuron and astrocyte co-culture. *Biochemical and Biophysical Research Communications*, *443*(4), 1176–1181. https://doi.org/10.1016/j.bbrc.2013.12.142

Odawara, Aoi, Gotoh, M., & Suzuki, I. (2013). A three-dimensional neuronal culture technique that controls the direction of neurite elongation and the position of soma to mimic the layered structure of the brain. *RSC Advances*, *3*(45), 23620. https://doi.org/10.1039/c3ra44757j

Peacock, J. H., Nelson, P. G., & Goldstone, M. W. (1973). Electrophysiologic study of cultured neurons dissociated from spinal cords and dorsal root ganglia of fetal mice. *Developmental Biology*, *30*(1), 137–152. https://doi.org/10.1016/0012-1606(73)90053-5

Pearson, K. (1901). LIII. On lines and planes of closest fit to systems of points in space. *The London, Edinburgh, and Dublin Philosophical Magazine and Journal of Science*, *2*(11), 559–572. https://doi.org/10.1080/14786440109462720

Pettersen, K. H., & Einevoll, G. T. (2008). Amplitude variability and extracellular low-pass filtering of neuronal spikes. *Biophysical Journal*, *94*(3), 784–802. https://doi.org/10.1529/biophysj.107.111179

Pfaff, S. L., Miranda, C. J., Zhu, M. X., Gage, F. H., Meyer, K., Kaspar, B. K., … Tian, J.

(2011). Rapid and Efficient Generation of Functional Motor Neurons From Human Pluripotent Stem Cells Using Gene Delivered Transcription Factor Codes. *Molecular Therapy*, *19*(10), 1905–1912. https://doi.org/10.1038/mt.2011.135

Pyka, M., Busse, C., Seidenbecher, C., Gundelfinger, E. D., & Faissner, A. (2011). Astrocytes are crucial for survival and maturation of embryonic hippocampal neurons in a neuron-glia cell-insert coculture assay. *Synapse*, *65*(1), 41–53. https://doi.org/10.1002/syn.20816

Quiroga, R. Q., Nadasdy, Z., & Ben-Shaul, Y. (2004). Unsupervised spike detection and sorting with wavelets and superparamagnetic clustering. *Neural Computation*, *16*(8), 1661–1687. https://doi.org/10.1162/089976604774201631

Raman, I. M., & Bean, B. P. (1997). Resurgent sodium current and action potential formation in dissociated cerebellar Purkinje neurons. *The Journal of Neuroscience : The Official Journal of the Society for Neuroscience*, *17*(12), 4517–4526. Retrieved from http://www.ncbi.nlm.nih.gov/pubmed/9169512

Rizk, M., & Wolf, P. D. (2009). Optimizing the automatic selection of spike detection thresholds using a multiple of the noise level. *Medical & Biological Engineering & Computing*, *47*(9), 955–966. https://doi.org/10.1007/s11517-009-0451-2

Sances, S., Bruijn, L. I., Chandran, S., Eggan, K., Ho, R., Klim, J. R., … Svendsen, C. N. (2016). Modeling ALS with motor neurons derived from human induced pluripotent stem cells. *Nature Neuroscience*, *19*(4), 542–553. https://doi.org/10.1038/nn.4273

Scain, A.-L., Le Corronc, H., Allain, A.-E., Muller, E., Rigo, J.-M., Meyrand, P., … Legendre, P. (2010). Glycine release from radial cells modulates the spontaneous activity and its propagation during early spinal cord development. *The Journal of Neuroscience : The*

*Official Journal of the Society for Neuroscience*, *30*(1), 390–403. https://doi.org/10.1523/JNEUROSCI.2115-09.2010

Schlaepfer, W. W. (1968). Acetylcholinesterase activity of motor and sensory nerve fibers in the spinal nerve roots of the rat. *Zeitschrift Fur Zellforschung Und Mikroskopische Anatomie (Vienna, Austria : 1948)*, *88*(4), 441–456. https://doi.org/10.1007/BF00571792

Schmidt, E. M. (1984). Computer separation of multi-unit neuroelectric data: a review. *Journal of Neuroscience Methods*, *12*(2), 95–111. https://doi.org/10.1016/0165-0270(84)90009-8

Segev, R., Goodhouse, J., Puchalla, J., & Berry, M. J. (2004). Recording spikes from a large fraction of the ganglion cells in a retinal patch. *Nature Neuroscience*, *7*(10), 1154–1161. https://doi.org/10.1038/nn1323

Silva, D. I., Santos, B. P. Dos, Leng, J., Oliveira, H., & Amédée, J. (2017). Dorsal root ganglion neurons regulate the transcriptional and translational programs of osteoblast differentiation in a microfluidic platform article. *Cell Death and Disease*, *8*(12). https://doi.org/10.1038/s41419-017-0034-3

Somogyvári, Z., Cserpán, D., Ulbert, I., & Érdi, P. (2012). Localization of single-cell current sources based on extracellular potential patterns: The spike CSD method. *European Journal of Neuroscience*, *36*(10), 3299–3313. https://doi.org/10.1111/j.1460-9568.2012.08249.x

Soriano, J., Rodriguez Martinez, M., Tlusty, T., & Moses, E. (2008). Development of input connections in neural cultures. *Proceedings of the National Academy of Sciences*, *105*(37), 13758–13763. https://doi.org/10.1073/pnas.0707492105

Southam, K. A., King, A. E., Blizzard, C. A., McCormack, G. H., & Dickson, T. C. (2013).

Microfluidic primary culture model of the lower motor neuron–neuromuscular junction circuit. *Journal of Neuroscience Methods*, *218*(2), 164–169. https://doi.org/10.1016/j.jneumeth.2013.06.002

Stark, E., & Abeles, M. (2007). Predicting movement from multiunit activity. *The Journal of Neuroscience : The Official Journal of the Society for Neuroscience*, *27*(31), 8387–8394. https://doi.org/10.1523/JNEUROSCI.1321-07.2007

Swindale, N. V., & Spacek, M. A. (2015). Spike detection methods for polytrodes and high density microelectrode arrays. *Journal of Computational Neuroscience*, *38*(2), 249–261. https://doi.org/10.1007/s10827-014-0539-z

Szabó, Z., Héja, L., Szalay, G., Kékesi, O., Füredi, A., Szebényi, K., … Kardos, J. (2017). Extensive astrocyte synchronization advances neuronal coupling in slow wave activity in vivo. *Scientific Reports*, *7*(1), 6018. https://doi.org/10.1038/s41598-017-06073-7

Takazawa, T., Croft, G. F., Amoroso, M. W., Studer, L., Wichterle, H., & Macdermott, A. B. (2012). Maturation of spinal motor neurons derived from human embryonic stem cells. *PloS One*, *7*(7), e40154. https://doi.org/10.1371/journal.pone.0040154

Taylor, A. R., Robinson, M. B., & Milligan, C. E. (2007). In vitro methods to prepare astrocyte and motoneuron cultures for the investigation of potential in vivo interactions. *Nature Protocols*, *2*(6), 1499–1507. https://doi.org/10.1038/nprot.2007.208

Thomas, C. A., Springer, P. A., Loeb, G. E., Berwald-Netter, Y., & Okun, L. M. (1972). A miniature microelectrode array to monitor the bioelectric activity of cultured cells. *Experimental Cell Research*, *74*(1), 61–66. https://doi.org/10.1016/0014-4827(72)90481-8

Tinkhauser, G., Pogosyan, A., Tan, H., Herz, D. M., Kühn, A. A., & Brown, P. (2017). Beta burst dynamics in Parkinson's disease off and on dopaminergic medication. *Brain*, *140*(11), 2968–2981. https://doi.org/10.1093/brain/awx252

Todorova, S., Sadtler, P., Batista, A., Chase, S., & Ventura, V. (2014). To sort or not to sort: The impact of spike-sorting on neural decoding performance. *Journal of Neural Engineering*, *11*(5). https://doi.org/10.1088/1741-2560/11/5/056005

Tomàs, J., Garcia, N., Lanuza, M. A., Santafé, M. M., Tomàs, M., Nadal, L., … Cilleros, V. (2017). Presynaptic Membrane Receptors Modulate ACh Release, Axonal Competition and Synapse Elimination during Neuromuscular Junction Development. *Frontiers in Molecular Neuroscience*, *10*(May), 1–12. https://doi.org/10.3389/fnmol.2017.00132

Trautmann, E. M., Stavisky, S. D., Lahiri, S., Ames, K. C., Kaufman, M. T., O'Shea, D. J., … Shenoy, K. V. (2019). Accurate Estimation of Neural Population Dynamics without Spike Sorting. *Neuron*, 1–17. https://doi.org/10.1016/j.neuron.2019.05.003

Umbach, J. A., Adams, K. L., Gundersen, C. B., & Novitch, B. G. (2012). Functional Neuromuscular Junctions Formed by Embryonic Stem Cell-Derived Motor Neurons. *PLoS ONE*, *7*(5), e36049. https://doi.org/10.1371/journal.pone.0036049

Ventura, V. (2008). Spike train decoding without spike sorting. *Neural Computation*, *20*(4), 923–963. https://doi.org/10.1162/neco.2008.02-07-478

Wagenaar, D. A., Pine, J., & Potter, S. M. (2006). An extremely rich repertoire of bursting patterns during the development of cortical cultures. *BMC Neuroscience*, *7*, 1–18. https://doi.org/10.1186/1471-2202-7-11

Wainger, B. J., Kiskinis, E., Mellin, C., Wiskow, O., Han, S. S. W. W., Sandoe, J., … Woolf, C. J. (2014). Intrinsic membrane hyperexcitability of amyotrophic lateral sclerosis patient-derived motor neurons. *Cell Reports*, *7*(1), 1–11. https://doi.org/10.1016/j.celrep.2014.03.019

Watkins, P. T., Santhanam, G., Shenoy, K. V, & Harrison, R. R. (2004). Validation of adaptive threshold spike detector for neural recording. *Conference Proceedings : ... Annual International Conference of the IEEE Engineering in Medicine and Biology Society. IEEE Engineering in Medicine and Biology Society. Annual Conference*, *6*, 4079–4082. https://doi.org/10.1109/IEMBS.2004.1404138

Weiss, P. (1945). Experiments on cell and axon orientation in vitro: The role of colloidal exudates in tissue organization. *Journal of Experimental Zoology*, *100*(3), 353–386. https://doi.org/10.1002/jez.1401000305

Xia, M., Zhu, S., Shevelkin, A., Ross, C. A., & Pletnikov, M. (2016). DISC1, astrocytes and neuronal maturation: a possible mechanistic link with implications for mental disorders. *Journal of Neurochemistry*, 518–524. https://doi.org/10.1111/jnc.13663

Yada, Y., Kanzaki, R., & Takahashi, H. (2016). State-Dependent Propagation of Neuronal Sub-Population in Spontaneous Synchronized Bursts. *Frontiers in Systems Neuroscience*, *10*(March), 1–13. https://doi.org/10.3389/fnsys.2016.00028

Yip, A. M., Ding, C., & Chan, T. F. (2006). Dynamic cluster formation using level set methods. *IEEE Transactions on Pattern Analysis and Machine Intelligence*, *28*(6), 877–889. https://doi.org/10.1109/TPAMI.2006.117

Zahavi, E. E., Ionescu, A., Gluska, S., Gradus, T., Ben-Yaakov, K., & Perlson, E. (2015). A

compartmentalized microfluidic neuromuscular co-culture system reveals spatial aspects of GDNF functions. *Journal of Cell Science*, *128*(6), 1241–1252. https://doi.org/10.1242/jcs.167544

Zhang, C., Zhang, X., Zhang, M. Q., & Li, Y. (2007). Neighbor number, valley seeking and clustering. *Pattern Recognition Letters*, *28*(2), 173–180. https://doi.org/10.1016/j.patrec.2006.07.003

Zhang, H., Wu, C.-Y., Wang, W., & Harrington, M. a. (2011). Interneuronal synapses formed by motor neurons appear to be glutamatergic. *NeuroReport*, *22*(16), 1. https://doi.org/10.1097/WNR.0b013e32834b6d5c